



U.S.-Pakistan

Centers for Advanced Studies in Water



Use of Multi-Level Remote Sensing to Evaluate Salinity on Irrigated Lands

Final Report 2019



Principal Investigator:

**Dr. Altaf Ali Siyal, U.S.-Pakistan Center for Advanced Studies in Water,
Mehran University of Engineering and Technology, Jamshoro, Pakistan**

Co-Principal Investigator:

**Dr. José L. Chávez, Civil and Environmental Engineering Department,
Colorado State University, USA**



MEHRAN UNIVERSITY
of Engineering & Technology
Jamshoro, Sindh, Pakistan



Citation

Siyal, A.A., and Chavez, J.L. (2019). Use of multi-level remote sensing to evaluate salinity on irrigated lands. U.S.-Pakistan Center for Advanced Studies in Water (USPCAS-W), MUET, Jamshoro, Pakistan

© All rights reserved by USPCAS-W. The authors encourage fair use of this material for non-commercial purposes with proper citation.

Authors

1. Dr. Altaf Ali Siyal, U.S.-Pakistan Center for Advanced Studies in Water, Mehran University of Engineering and Technology, Jamshoro, Pakistan
2. Dr. Jose L. Chavez, Civil and Environmental Engineering Department, Colorado State University, USA

ISBN

978-969-7970-01-8

Acknowledgment

This work was made possible by the support of the United States Government and the American people through the United States Agency for International Development (USAID).

Disclaimer

The contents of the report are the sole responsibility of the authors and do not necessarily reflect the views of the funding agency and the institutions they work for.



USAID
FROM THE AMERICAN PEOPLE

U.S.-Pakistan

Centers for Advanced Studies in Water

Use of Multi-Level Remote Sensing to Evaluate Salinity on Irrigated Lands

Final Report 2019



Principal Investigator:

**Dr. Altaf Ali Siyal, U.S.-Pakistan Center for Advanced Studies in Water,
Mehran University of Engineering and Technology, Jamshoro, Pakistan**

Co-Principal Investigator:

**Dr. José L. Chávez, Civil and Environmental Engineering Department,
Colorado State University, USA**



MEHRAN UNIVERSITY
of Engineering & Technology
Jamshoro, Sindh, Pakistan



TABLE OF CONTENTS

ACKNOWLEDGMENTS	vi
ACRONYMS AND ABBREVIATIONS	vii
EXECUTIVE SUMMARY.....	viii
1. INTRODUCTION.....	1
1.1 Background	1
1.2 Monitoring and Measurement of Soil Salinity.....	1
1.3 Rationale/Research Gaps to be Filled	2
1.4 Aim and Objectives	3
1.4.1 Objectives	3
1.5 Expected Results/ Outcome	3
1.6 Beneficiaries of the Study	3
1.7 Limitations	4
2. MATERIALS AND METHODS.....	5
2.1 Study Area	5
2.1.1 Deshak agricultural farm (Rohri canal command area).....	5
2.1.2 Aamir agricultural farm (Nara canal command area)	5
2.2 Vegetation Index (VI) for Detecting Soil Salinity in Bare Soils and Vegetated (cropped) Areas	6
2.2.1 Top of atmospheric correction	7
2.2.2 Vegetation indices.....	7
2.3 Field Determinations	10
2.3.1 Soil salinity	10
2.3.2 Soil texture and dry bulk density.....	13
2.3.3 Soil moisture measurement	13
2.3.4 Monitoring of groundwater table depth	14
2.3.5 Image classification.....	14
2.3.6 Climatic data	15
2.3.7 Reflectance with a multispectral radiometer (MSR)	15
2.4 Remote Sensing (RS) for Actual Crop Water Use	15
2.4.1 Crop phenology and yield	16
2.4.2 ETa and soil salinity.....	16
3. RESULTS AND DISCUSSIONS	17
3.1 Soil Texture	17
3.2 Moisture Content	17
3.3 Soil Salinity.....	20
3.3.1 Experimental field-I	20
3.3.2 Experimental field-II	23
3.4. Water Table and Irrigation	24

3.4.1	Irrigation	24
3.4.2	Water table	26
3.5	Vegetation Indices	28
3.6	Multispectral Radiometer (MSR) Reflectance	28
3.7	Crop Phenology	30
3.7.1	Plant biomass	31
3.7.2	Plant height	31
3.8	Cotton Yield	32
3.8.1	Cotton	32
3.9	Research Output	33
3.9.1	M.E. Thesis	33
3.9.2	Conference/seminar presentations	33
4.	Conclusion and Recommendations.	34
4.1	Conclusions	34
4.2	Recommendations	35
	REFERENCES	36

LIST OF FIGURES

Fig. 2.1:	Location map of the experimental field-I	5
Fig. 2.2:	Location map of the experimental field-II	6
Fig. 2.3:	Equipment used for the EMI survey	10
Fig. 2.4:	Glimpses of EMI survey	11
Fig. 2.5:	Sampling scheme of soil apparent electrical conductivity (EC_a) measurements and soil sampling locations for EC_e	11
Fig. 2.6:	ESAP-95 software bundle: Program flowchart	12
Fig. 2.7:	Soil sampling locations for moisture content determinations	14
Fig. 2.8:	Flow chart of the supervised classification	14
Fig. 2.9:	Measuring the light reflectance through MSR	15
Fig. 2.10:	Methodology flow diagram.	16
Fig. 3.1:	Spatial distribution of soil texture at (a) 0-20 cm, (b) 20-40 cm, (c) 40-60 cm, and (d) 60-80 cm soil depths at Deshak Agricultural Farm (Experimental Field-I)	17
Fig. 3.2:	Spatial distribution of soil texture at (a) 0-20 cm, (b) 20-40 cm, (c) 40-60 cm, and (d) 60-80 cm soil depths at Aamir Agricultural Farm (Experimental Field-II)	18
Fig. 3.3:	2-D and 3-D view of the spatial distribution of soil moisture in 0-20 cm soil depth after (a) 2 days (b) 10 days, and (c) 15 days after irrigation at Deshak Agricultural Farm (Experimental Field-I).	18
Fig. 3.4:	2-D and 3-D view of the spatial distribution of soil moisture after (a) 2 days (b) 10 days, and (c) 15 days of irrigation at 0-20 cm soil depth at Aamir Agricultural Farm (Experimental Field-II).	19
Fig. 3.5:	Spatial distribution of apparent electrical conductivity (EC_a) of 0.75 m layer of Deshak Agricultural Farm (Experimental Field-I) obtained through EMI survey and plotted using (a) SaltMapper and (b) Surfer 16	20
Fig. 3.6:	Spatial distribution of apparent electrical conductivity (EC_a) of 1.5 m soil layer of Deshak Agricultural Farm (Experimental Field-I) obtained through EMI survey and plotted using (a) SaltMapper 3.5 and (b) ArcGIS 10.5	21
Fig. 3.7:	Spatial distribution of predicted electrical conductivity of soil saturated extract (EC_e) of 0.8 m soil layer of Deshak Agricultural Farm (Experimental Field-I) predicted from ESAP-Calibrate 3.5 and plotted using SaltMapper 3.5	22
Fig. 3.8:	Relationship between EC_a and EC_e	22
Fig. 3.9:	Spatial distribution of apparent electrical conductivity (EC_a) of 0.75 m layer of Aamir Agricultural Farm (Experimental Field-II) obtained through EMI survey and plotted using (a) SaltMapper and (b) Surfer 16	23

Fig. 3.10:	Spatial distribution of apparent electrical conductivity (EC_a) of 1.5 m soil layer of Aamir Agricultural Farm (Experimental Field-II) obtained through EMI survey and plotted using SaltMapper 3.5.	24
Fig. 3.11:	Depth of rainfall and irrigation water applied to the mustard crop at Experimental Field-I	25
Fig. 3.12:	Depth of rainfall and irrigation water applied to the cotton crop at the Experimental Field-I	25
Fig. 3.13:	Depth of irrigation water applied to the mustard crop at Experimental Field-II. . .	26
Fig. 3.14:	Depth of irrigation water applied to the cotton crop at Experimental Field-II	26
Fig. 3.15:	Temporal fluctuation in the water table depth at the Experimental Field-I.	27
Fig. 3.16:	Temporal fluctuation in the water table depth at the Experimental Field-II	27
Fig. 3.17:	Temporal and spatial variation in the NDVI for the mustard crop at Experimental Field-I (a) Nov. 18, 2018 (b) Dec. 18, 2018 (c) Jan. 18, 2019. . . .	28
Fig. 3.18:	Temporal variation in NDVI for the mustard crop at Experimental Field-I (a) Nov. 03, 2018 (b) Nov. 18, 2018 (c) Dec. 05, 2018 (d) Dec. 18, 2018 (e) Jan. 3, 2019 and (f) Jan. 18, 2019.	29
Fig. 3.19:	Temporal variation in NDVI for the mustard crop at Experimental Field-I for low, medium and high salinity	29
Fig. 3.20:	Light reflectance (%) from the mustard field in different bands from the low, medium, and high salinity levels (a) Nov. 03, 2018 (b) Nov. 18, 2018 (c) Dec. 05, 2019 (d) Dec. 18, 2019 (e) Jan. 03, 2019 and (f) Jan. 18, 2019	30
Fig. 3.21:	Cotton crop biomass per plant obtained from locations with low, medium and high salinity levels	31
Fig. 3.22:	Height of cotton plants grown at locations with low, medium and high salinity levels	31
Fig. 3.23:	Crop yield obtained from locations with low, medium and high salinity levels. . .	32

LIST OF ANNEXURES

Annexure-1	41
1.1 Climatic data for October 2018	41
1.2 Climatic data for November 2018	42
1.3 Climatic data for December 2018	43
1.4 Climatic data for January 2019	44
1.5 Climatic data for February 2019	45
1.6 Climatic data for March 2019	46
1.7 Climatic data for April 2019	47
1.8 Climatic data for May 2019	48
1.9 Climatic data for June 2019	49
1.10 Climatic data for July 2019	50
1.11 Climatic data for August 2019	51
1.12 Climatic data for September 2019	52

ACKNOWLEDGMENTS

The authors gratefully acknowledge the United States Agency for International Development (USAID) for funding this project through the U.S.-Pakistan Center for Advanced Studies in Water (USPCAS-W), Mehran University of Engineering & Technology (MUET), Jamshoro, Pakistan under the Applied Policy Research Grants. Technical training and assistance provided by Dr. A.J. Brown, Prof. Allan Andales, and Prof. Tim Gates, University of Colorado, USA, are highly appreciated and acknowledged.

Active participation in implementation of the project plans and in data collection and analysis by Kashif Solangi and Kamran Khan Phulan, Research Assistants, and Sarwan Nahiyoon, MS student, is highly commendable. Support, encouragement, and inspiration of Dr. Kazi Suleman Memon, Manager Research, USPCAS-W, MUET Jamshoro, during the entire project period, is highly acknowledged. Besides, the support provided by Aami Bhatti and Zulfiqar Deshak in providing the agricultural land for conducting the experimental study and during the collection of data is also highly appreciated and acknowledged.

Moreover, Planet.com, United States Geological Survey (USGS), National Aeronautics and Space Administration (NASA), Drainage and Reclamation Institute of Pakistan (DRIP), and Google Earth are also acknowledged for offering free of cost fine resolution imagery, historic satellite imagery, Digital Elevation Model (DEM), meteorological data and other spatial data, respectively.

ACRONYMS AND ABBREVIATIONS

AOI	Area of Interest
CRS	Crop Reporting Services
DN	Digital Numbers
dS/m	Deci Siemens per meter
EC _a	Apparent Electrical Conductivity of Soil
EC _e	Electrical Conductivity of the Soil Saturation Extract
ESAP	Electrical Conductivity, Sampling, Assessment, and Prediction
ESP	Exchangeable Sodium Percentage
GIS	Geographical Information System
GPS	Global Positioning System
ha	Hectare
LST	Land Surface Temperature
MAF	Million Acre Feet
mg	Milligrams
mg/L	Milligrams/Liter
MSR	Multispectral Radiometer
NDSI	Normalized Difference Salinity Index
NDVI	Normalized Difference Vegetation Index
NIR	Near Infrared
PMD	Pakistan Meteorological Department
R ²	Coefficient of Determination
SAR	Sodium Adsorption Ratio
TOA	Top of Atmospheric Correction
USGS	United States Geological Survey

EXECUTIVE SUMMARY

Soil salinization is the accumulation of soluble salts at or near the soil surface affecting soil properties and crop yield, especially under arid and semi-arid environments. In Sindh, nearly 40% of soils are affected by salinity, which is robbing 25-40 percent of crop production in the province. The studies about the identification of the degree of salinity relating to spatial effects on crop water use and yield are vital for the evaluation of the economic impacts of soil salinization on crop productivity. To date, no efficient and quick methodology has been adopted to effectively monitor and map the soil salinity in the province of Sindh using multispectral satellite data to quantify the spatial effects of soil salinity on crop yield. This study was conducted using field, satellite, and multispectral data to quantify the severity of the salinity and its impact on crop yield. The overall aim of the study was to discover effective and economic remotely-sensed indicators to identify and map not only the presence of soil salinity but also the degree of salinity and severity of its impact on crop water use and yield.

The study was conducted during 2018 and 2019 on two experimental fields located in districts Tando Allahyar and Mirpur Khas. PlanetScope Satellite data with four bands, visible (blue, green, and red) and near-infrared, were used because of the high spatial and temporal resolution. The imagery was clipped to extract the area of interest (AOI) from the scene and then atmospherically corrected. Different vegetation indices were calculated from the imagery collected at regular intervals during the entire growing season. Multispectral radiometer (MSR) readings were also collected during the pass of the satellite from the selected locations and were compared with the reflectance of the satellite image pixel under observation. Soil texture down to 80 cm was determined from the randomly collected soil samples from each experimental field. These samples were also analyzed for electrical conductivity of the saturated extract (EC_e), pH, and exchangeable sodium percentage (ESP) before the experiment. The status of soil salinity of both of the experimental fields was also determined through electromagnetic induction (EMI) survey using EM38-Mk2. The EMI data were processed using electrical conductivity, sampling, assessment, and prediction (ESAP) software for apparent electrical conductivity (EC_a) and sampling design locations for soil sampling needed for calibration to convert EC_a into EC_e . ESAP and ArcGIS 10.5 softwares were also used for spatial mapping of the soil salinity.

The mustard crop was sown on both fields during Rabi season by the farmers, while for Kharif season cotton crop was grown. Water table depth was continuously monitored for both growing seasons through weekly readings of installed piezometers. Also, moisture content down to 80 cm depth was measured by the gravimetric method at regular time intervals for both the experimental fields. The rainfall and other climatic

data were obtained from DRIP, Tandojam. The irrigation water applied by farmers to Kharif and Rabi crops grown in both fields was measured each time using cut-throat flume.

The results of the study revealed that the soil texture of both of the fields was medium to heavy, dominated by silty clay loams and clayey textures. The soils at both locations had enough water holding capacity such that even after 15 days after irrigation, the soil had sufficient moisture content to support the crop growth. The apparent soil electrical conductivity (EC_a) at Field-I ranged from 2.8 to 8.5 dS/m. The plots depicted that the EC_a was higher along the edge of the eastern side of the field, while central areas had lower EC_a . While for the Field-II, the EC_a ranged from 3 to 7.3 dS/m. The EC_a values were higher along the edge of the eastern side and a small portion of the central area of the field. The EC_a - EC_e correlation plots showed that EC_a values were slightly smaller than the EC_e values, which reflects that EM38-MK2 underestimated soil salinity. It might be due to the impact of soil water content (SWC) being less than the field capacity.

The irrigation water used for the mustard crop was 411.6 mm and 384 mm for Field-I and Field-II, respectively. While it was 954 mm and 970 mm for the cotton crop for Field-I and Field-II, respectively. The continuous monitoring of the groundwater table revealed that the water table depth fluctuated between 3.75 and 4.6 m depths at the Field-I while it varied between 1.75 and 2.4 m at the Field-II.

The NDVI ranged from 0.17 to 0.59 during the peak growth of the mustard crop. The NDVI values were always high for low salinity locations, whereas the locations with high soil salinity had lower NDVI values throughout the crop growth period. The mustard crop yield decreased tremendously such that at medium ($EC = 2-5$ dS/m) and high soil salinity ($EC > 5$ dS/m) crop yield decreased by 11.6% and 31.3%, respectively. The cotton crop yield response to salinity for Field-I at a low saline area varied from 0.39 to 0.42 kg/m² with an average of 0.40 ± 0.015 kg/m². The yield values at medium saline soil fluctuated between 0.19 to 0.38 kg/m² with an average of 0.285 ± 0.05 kg/m² and at high saline varied from 0.06 to 0.17 kg/m² with an average of 0.12 ± 0.03 kg/m².

The study concludes that the soil salinity and the crop response to varying degrees of soil salinity can be monitored using multi-level remotely sensed data. It is recommended to use the remotely sensed data for the prediction of the crop yields from the agricultural fields of Pakistan with varying degrees of soil salinity.

1. INTRODUCTION

1.1 Background

Soil salinization is the buildup of soluble salts at or near the soil surface, adversely affecting soil properties and crop production (Siyal *et al.*, 2002; Abbas *et al.*, 2013). It is a world-wide issue of arid and semi-arid regions wherever irrigated agriculture is practiced (Metternicht, 2003; Yao and Yang, 2010) and threatens the sustainability and reliability of food production systems (Lobell, 2010). Soil salinity hinders plant growth, reduces crop production, deteriorates the soil and water quality, and sometimes results in abandoning of cultivation of land (Zhu, 2001; Gorji, 2015). Globally, it is estimated that about 0.34×10^9 ha (23%) of cultivated lands are saline, while 0.56×10^9 ha (37%) are sodic (Wallender and Tanji, 2012). Soil salinity is spreading throughout the world at a rate of up to 2 Mha a year, which offsets the increased crop yields obtained through expanding irrigation (Postel, 1999), quoted by Eldiery *et al.* (2005).

Soil salinity is one of the most devastating agro-environmental issues affecting crop growth and thereby threatening the sustainability of agriculture in Pakistan. About 6.67 Mha or 8% of the total geographic area is salt-affected in Pakistan (Khan, 1998), including about 30% of irrigated lands (Qureshi, 2011). In Sindh province, out of 5.45 Mha of irrigated land, 2.321 Mha (or 42%) are salt-affected (Alam and Ansari, 2000).

Secondary soil salinization or human-induced salinization is caused due to the upward movement of salts present in the soil profile as a result of human activities such as irrigation (Szabolcs, 1989). Inefficient flood irrigation methods, saline irrigation water, shallow saline groundwater, arid climate, high temperature, and seepage from canals are some primary causes of salinization in Pakistan. The severity of the irrigation-induced soil salinity menace is more prominent in Pakistan's southern Sindh province, having about 5.45 Mha of irrigated land, of which nearly 40% is affected by soil salinity and water shortage. It is reported that soil salinity is robbing 25-40 percent of crop production in the province of Sindh alone.

1.2 Monitoring and Measurement of Soil Salinity

Soil salinization is categorized by its development in both time and space (Abbas *et al.*, 2013). Hence, the monitoring and assessment of its extent and severity are important to developing potential solution strategies at local and regional scales. The use of conventional methods (collection of *in-situ* soil samples and laboratory analysis) for its monitoring is not so practical since it is costly, labor-intensive, and time-consuming. Remote sensing (RS) data and tools have been applied to monitor and map salt-affected areas since the 1960s (Dale *et al.*, 1986). Soil salinity usually is

detected either directly from remotely sensed visible spectra data through the visible salt crust at the soil surface (Teggi *et al.*, 2012; Matnifar *et al.*, 2013) or indirectly from indicators of salt-affected soils such as the presence of halophytic plants (Aldakheel, 2011). The delineating, monitoring, and mapping of saline soils, using remotely-sensed data integrated with GIS techniques, has been reported as more reliable, economical, rapid, and efficient (Srivastava *et al.*, 1997; Dwividi *et al.*, 1998). It is more common to find studies, like that of Abbas *et al.* (2013), characterizing soil salinity in irrigated agriculture using a remote sensing approach to classify percentages of land affected by salt. Abbas *et al.* (2013) found that the total land affected by salts in the Faisalabad district of Punjab in Pakistan during 1992 was about 22.2% (including 15% slightly saline, 3% moderately saline, and 1% strongly saline soils). This study (like several others) does not address the salt concentration and corresponding spatial effects on crop production. Methods to date have struggled to provide information that distinguishes varying levels of salinization over broad regions (Metternicht and Zinck, 2003; Allbed and Kumar, 2013).

1.3 Rationale/Research Gaps to be Filled

As evident from the literature, no methodology has so far been developed to effectively monitor and map soil salinity in the Sindh province using multi-level and multispectral satellite data and quantify the spatial effects of soil salinity on crop water requirements and yield. Such studies are essential for the evaluation of the economic impacts of soil salinization on crop productivity for the sake of prioritization of investment needed for remedial measures. The development of salinity-related crop production functions would be instrumental in identifying sub-areas, crops, and irrigation management for the economic benefit of farming communities. With the information so gained, a better allocation of scarce resources will be possible to optimize economic crop production. Severity maps of salt-affected soils also can be used to estimate the amount of water (of varying quality) that may be needed to reclaim or improve areas affected at different salt concentrations.

Herein, a study was conducted that combined the use of the thermal infrared (TIR) spectrum in conjunction with multiple visible (VIS), near infra-red (NIR) and mid-infrared (MIR) spectra from near-ground (hand-held radiometer) and remote (satellite cameras) levels, ground-validated with field measurements of soil and crop characteristics, to characterize salinization and crop water use and stress in irrigated regions. Spatial data from the TIR, VIS, and NIR bands were processed to estimate actual crop evapotranspiration (ET_a) and crop water stress indices, following selected remote sensing of ET_a algorithms (e.g., Bastiaanssen *et al.*, 1998a, b; Kustas and Norman, 2000; Elhaddad *et al.*, 2010; Mkhwanazi *et al.*, 2015) which vary with degrees

of soil osmotic potential depression brought about by different degrees of salinization (Wallender and Tanji, 2012; Gates *et al.*, 2012) along with varying levels of soil water deficit. The work was done on representative field sites in the Rohri and Nara Canal Command area of Sindh. The study was carried out in conjunction with a similar field project in the irrigated Arkansas River Valley of Colorado, USA.

1.4 Aim and Objectives

The overall aim of this project was to discover effective and economic remotely-sensed indicators to identify and map not only the presence of salinity but also the level of salinity and the severity of its impact on crop water use and yield, in a pilot study area with a long-term outlook toward application across irrigated regions of Pakistan.

1.4.1 Objectives

1. Determine which vegetation index (VI) is most effective in detecting salinity presence in bare soils and vegetated (cropped) areas throughout the crop growing season.
2. Determine which remote sensing (RS) of the ET_a algorithm is effective and consistent in spatially quantifying salinity concentration, actual crop water use, the reduction of crop water use, and crop yield reduction due to a range of soil salt concentration.

1.5 Expected Results/ Outcome

- a. Determination of an effective and suitable vegetation index (VI) for delineation of soil salinity both on barren land and cropped land
- b. Determination of a suitable spatial ET_a algorithm effective and consistent in using remotely-sensed data to quantify salt concentration, the reduction of crop water use, and crop yield degradation due to a range of soil salt concentration under arid climate.

1.6 Beneficiaries of the Study

The beneficiaries of the study will be:

- i. Policymakers
- ii. Teaching and research institutes
- iii. Farming community residing in delta
- iv. Environmental agencies
- v. Irrigation and water management professionals
- vi. Local NGOs working on land degradation

1.7 Limitations

Following are the limitations/constraints of the study:

- ☐ Equipment such as EM38-MK2 and MSR
- ☐ ESAP and GIS/Remote sensing software
- ☐ Bright and clear weather for getting remote sensing data

2. MATERIALS AND METHODS

This study was conducted during 2018 and 2019 on two experimental fields located in the Rohri and Nara canal command areas in districts Tando Allahyar and Mirpur Khas, respectively.

2.1 Study Area

2.1.1 Deshak agricultural farm (Rohri canal command area)

The first site, Deshak Agricultural Farm, is located at longitude 68°53'54.99"E and latitude 25°20'56.51"N at an elevation of about 20 m above mean sea level, near Chambar, district Tando Allahyar (Fig. 2.1). The area of the experimental field is 9 acres (3.6 ha). The field receives irrigation water from the Naseer canal, a sub-canal of the Rohri canal. The area falls in an arid region, which receives less than 200 mm of rainfall annually. The climate of the area is hot during summer with temperatures up to 48°C while it is cold during winter with an average winter temperature of 11°C, sometimes temperature falls to 0°C. The cotton and sugarcane are the major Kharif crops while wheat and vegetables are grown during the Rabi period.

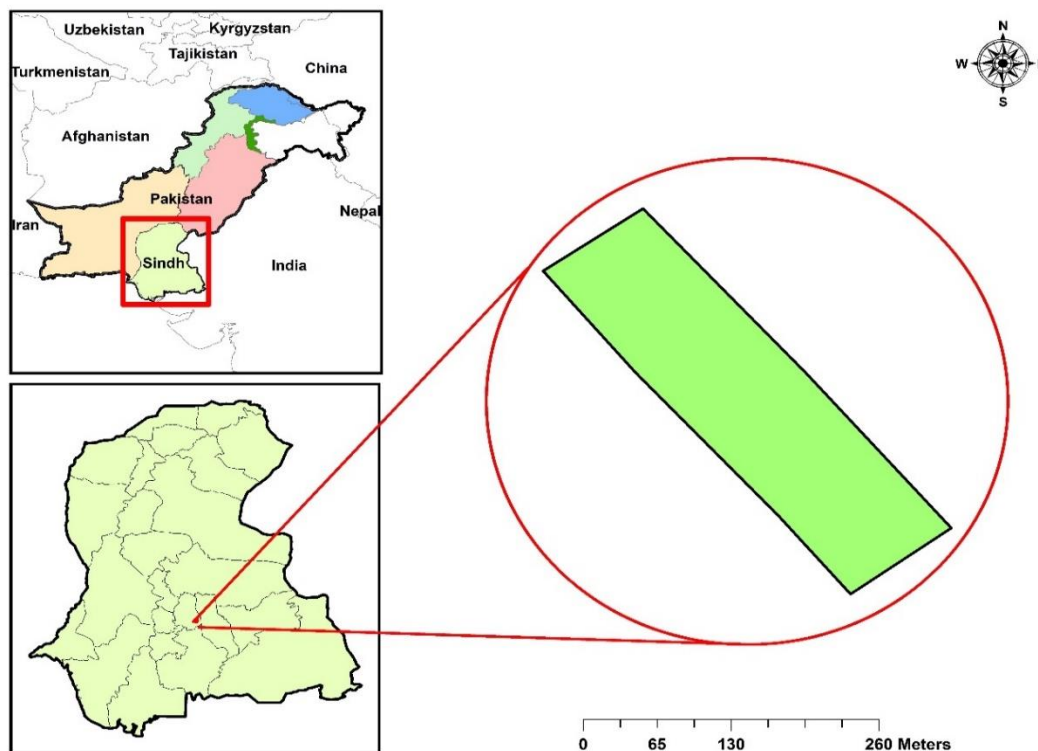


Fig. 2.1: Location map of the experimental field-I

2.1.2 Aamir agricultural farm (Nara canal command area)

The second experimental field, Aamir Agricultural Farm, is located at longitude 69°19'22.57"E and latitude 25°14'8.39"N at an elevation of about 12 m above mean sea level, near Kot Ghulam Muhammad, district Mirpur Khas (Fig. 2.2). The

experimental field, measuring 21.4 acres (8.66 ha) is located at the tail end of the Nara canal command area. It gets irrigation water from the Jamrao canal, a sub-canal of the Nara canal. The area falls within an arid region where annual rainfall is less than 200 mm. The climate of the area is hot during summer, reaching temperatures up to 45°C while it is cold during winter, with an average winter temperature of 12° C (sometimes temperature falls to 2°C). Cotton and wheat are the major Kharif and Rabi crops, respectively, while mango orchards are also spread on vast fields in the district Mirpur Khas.

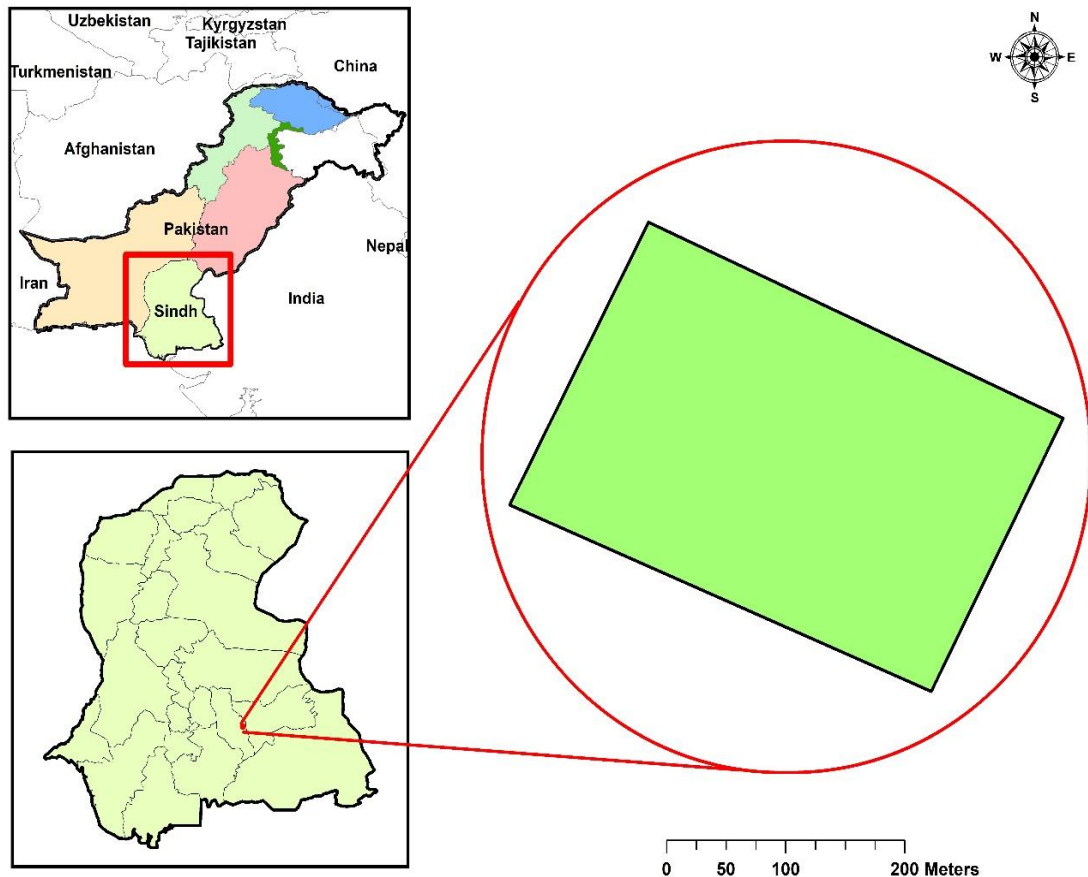


Fig. 2.2: Location map of the experimental field-II

2.2 Vegetation Index (VI) for Detecting Soil Salinity in Bare Soils and Vegetated (cropped) Areas

To address the first objective, several vegetation indices, using surface reflectance from bands in the visible and near infra-red range, in combination with the thermal band derived surface temperature, were atmospherically corrected to identify areas affected by salinity through the supervised classification method in a GIS environment. For the study, PlanetScope satellite data with four bands, visible (blue, green, and red) and near-infrared, were used because of the high spatial (3 m) and temporal (daily) resolution of PlanetScope compared to Sentinel-2 and Landsat data. While for thermal emissions, Landsat data were used. The PlanetScope data were downloaded from the

planet.com website. Satellite imagery of 3 m resolution for Nov. 03 and 18, 2018; Dec. 05 and 18, 2018; Jan. 03 and 18, 2019; and Feb. 04, 2019, were downloaded. The imagery was clipped with the shapefile of the study areas, i.e., Field-I and Field-II, to extract the areas of study from the entire scene.

2.2.1 Top of atmospheric correction

All bands of the extracted images were first atmospherically corrected by multiplying the reflectance coefficients (provided in metadata file) of the bands with digital numbers (DN) of the respective rasters using the MapAlgebra tool in ArcGIS 10.5. The atmospherically corrected imagery was then used for further analysis. Vegetation indices used in the present study are described in the subsequent section.

2.2.2 Vegetation indices

2.2.2.1 Normalized difference vegetation index (NDVI)

NDVI is a measure of the health and greenness of vegetation. The combination of its normalized difference formulation and use of the highest absorption and reflectance regions of chlorophyll makes it robust over a wide range of conditions. It can, however, saturate in dense vegetation conditions when LAI becomes high. The NDVI values range between -1 and 1. The normal range for green vegetation is between 0.2 and 0.8.

$$NDVI = \frac{NIR - RED}{NIR + RED} \quad (\text{Rouse } et al., 1973)$$

2.2.2.2 Optimized soil adjusted vegetation index (OSAVI)

This vegetation index takes a standard value of 0.16 for the canopy background adjustment factor. Rondeaux *et al.* (1996) found that this value provides greater soil variation than SAVI for low vegetation cover while demonstrating increased sensitivity to vegetation cover greater than 50%. The index is best suited for areas with relatively sparse vegetation with visible soil through the canopy.

$$OSAVI = (1 + 0.16) \frac{NIR - RED}{NIR + RED + 0.16} \quad (\text{Rondeaux } et al., 1996)$$

2.2.2.3 Ratio-based vegetation index (RVI)

Jordan (1969) proposed one of the first vegetation indices, Ratio Vegetation Index (RVI), which is based on the principle that plant leaves absorb relatively more red than infrared light; RVI can be expressed mathematically as:

$$RVI = \frac{NIR}{RED} \quad (\text{Jordan, 1969; Major } et al., 1990)$$

2.2.2.4 Infrared percentage vegetation index (IPVI)

This index is the ratio of near-infrared and a combination of both near-infrared and red bands. It is functionally the same as NDVI, but it is computationally faster. The values of the index range between 0 and 1.

$$IPVI = \frac{NIR}{NIR + RED} \quad (\text{Crippen et al., 1990})$$

2.2.2.5 Green ratio vegetation index (GRVI)

The green ratio vegetation index is sensitive to photosynthetic rates in vegetation canopies because leaf pigments strongly impact the energy reflected in green and red bands.

$$GRVI = \frac{NIR}{GREEN} \quad (\text{Sripada et al., 2006})$$

2.2.2.6 Enhanced vegetation index (EVI)

This vegetation index was originally developed for use with MODIS data as an improvement over NDVI by optimizing the vegetation signal in areas of high leaf area index (LAI). It is most useful in high LAI regions where NDVI may saturate.

$$EVI = 2.5 * \frac{NIR - RED}{NIR + 6 * RED - 7.5 * BLUE + 1} \quad (\text{Huete et al., 2002})$$

The EVI values range between -1 and 1

2.2.2.7 Leaf area index (LAI)

The leaf area index (LAI) is used to estimate vegetation cover and to forecast crop growth and yield. High LAI values usually range from approximately 0 to 3.5. However, when the area contains clouds and other bright features that produce saturated pixels, the LAI values sometimes exceed the value of 3.5. Therefore, it is required to mask out clouds and other bright features from the scene before determining LAI from the image. LAI can be calculated using the following empirical formula:

$$LAI = 3.168 * EVI + 0.118 \quad (\text{Boegh et al., 2002})$$

2.2.2.8 Soil adjusted vegetation index (SAVI)

The index is similar to NDVI, but it suppresses the impact of soil pixels. It uses a canopy background adjustment factor, L , which depends on vegetation density. Huete (1988) proposed an optimal value of $L=0.5$ to account for first-order soil background variations. The index is best suited for areas with relatively sparse vegetation where the soil is visible through the canopy.

$$SAVI = \frac{1.5 * (NIR - RED)}{(NIR + RED + 0.5)} \quad (\text{Huete, 1988})$$

2.2.2.9 Difference vegetation index (DVI)

The difference vegetation index (DVI) differentiates between soil and vegetation, but it does not account for the difference between reflectance and radiance caused by atmospheric effects or shadows.

$$DVI = NIR - RED \quad (\text{Tucker, 1979})$$

2.2.2.10 Modified soil adjusted vegetation index (MSAVI)

This index improves upon the soil adjusted vegetation index (SAVI). It reduces soil noise and increases the dynamic range of the vegetation signal. MSAVI is based on an inductive method to highlight green vegetation.

$$MSAVI = \frac{2 * NIR + 1 - \sqrt{(2 * NIR + 1)^2 - 8(NIR - RED)}}{2} \quad (\text{Qi et al., 1994})$$

2.2.2.11 Wide dynamic range vegetation index (WDRVI)

This vegetation index is similar to NDVI, but it uses a weighting coefficient (a) to reduce the disparity between the contributions of the near-infrared and red signals to the NDVI. The WDRVI is useful in areas that have moderate-to-high vegetation density, with the value of NDVI more than 0.6. NDVI tends to level off when vegetation fraction and leaf area index (LAI) increase, whereas the WDRVI is more sensitive to a wider range of vegetation fractions and changes in LAI. The weighting coefficient (a) can range from 0.1 to 0.2. We used a value of 0.2, as recommended by Henebry *et al.* (2004).

$$WDRVI = \frac{a * NIR - RED}{a * NIR + RED} \quad (\text{Gitelson, 2004})$$

2.2.2.12 Canopy response salinity index (CRSI)

The canopy response salinity index (CRSI) has been highly successful for mapping regional-scale salinity in the USA. The CRSI is mathematically defined as:

$$CRSI = \sqrt{\frac{(NIR * R) - (G * B)}{(NIR * R) + (G * B)}} \quad (\text{Scudiero et al., 2014})$$

The higher CRSI value reflects a vigorous plant. The CRSI is not a salinity-specific vegetation index; it was selected by Scudiero *et al.* (2015) because it provided better performance than other vegetation indices when applied to their salinity ground-truthing calibration data

2.3 Field Determinations

2.3.1 Soil salinity

2.3.1.1 Electromagnetic induction survey (EMI)

Soil salinity was estimated through electromagnetic induction survey (EMI) using an electromagnetic induction sensor (Geonics EM38-MK2). The complete set of EM38-MK2 data-logging system contains EM38-MK2 equipment for getting electromagnetic induction data, Geode for GPS-located measurements, and Archer (Fig. 2.3).



Fig. 2.3: Equipment used for the EMI survey

During the EMI survey, EM38-MK2 and Archer were carried in hands while Geode in the backpack during moving in the field. EM38-MK2 recorded the apparent soil salinity (EC_a) of the profile down to 1.5 m depth while Geode, connected with satellite, provided the coordinates of the sampling locations. Both EC and sampling locations were recorded in real-time and stored in the Archer (Fig. 2.4). The EMI surveys of both experimental fields were conducted before the sowing and harvesting of the crop.

The GPS-located measurements of the apparent bulk electric conductivity (EC_a) were conducted in the zigzag sampling scheme as per the guidance manual of the equipment and its data processing software, i.e., electrical conductivity, sampling, assessment, and prediction (ESAP) (Lesch *et al.* 1995, 2000) as shown in Fig. 2.5. At all survey points, two EM readings were done, one with the coil of the EM38-MK2 device positioned horizontally to the soil surface (EMh) and the second one with the device positioned vertically (EMv). These readings were performed a few days after an irrigation event, i.e., when the soil water content was close to field capacity. The soil temperature was measured at depths of 20 and 40 cm to convert EM38 readings to

the reference temperature of 25°C. The EM38 readings were mapped with the ESAP SaltMapper program (Lesch *et al.*, 2002b), which employs inverse-distance-squared (IDS) interpolations.



Fig. 2.4: Glimpses of EMI survey

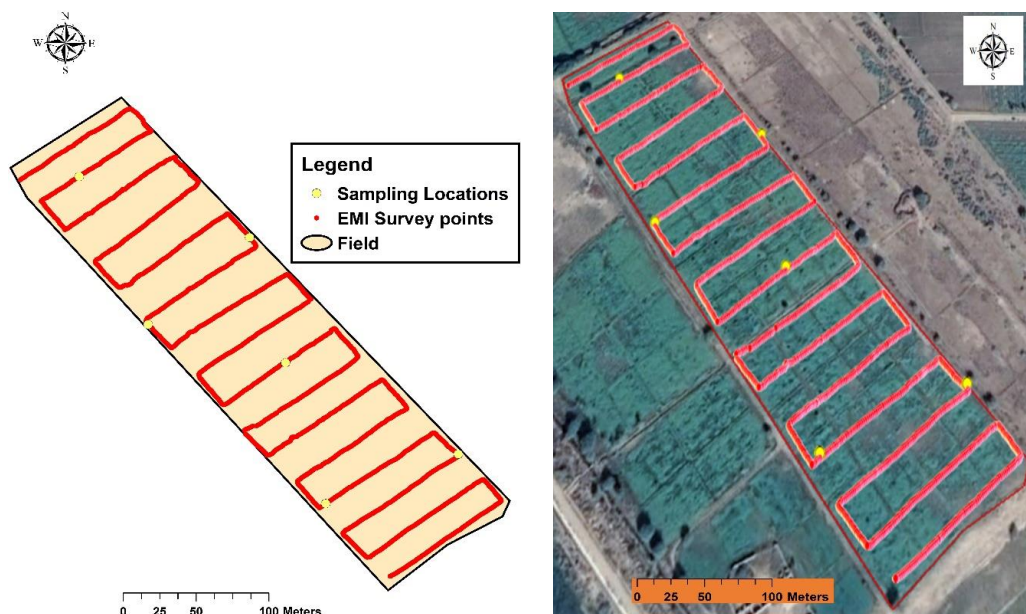


Fig. 2.5: Sampling scheme of soil apparent electrical conductivity (EC_a) measurements and soil sampling locations for EC_e

The EC_a measurements were then calibrated with an analysis of soil samples from monitoring points selected using the ESAP method. The complete process of data analysis with ESAP software is summarized in the flow chart shown in Fig. 2.6. Soil temperature and soil water content measurements were used in calibrating EC_a against EC of soil extract (EC_e) (Rhoades, 1996; Wittler *et al.*, 2006) that can be correlated to crop yield.

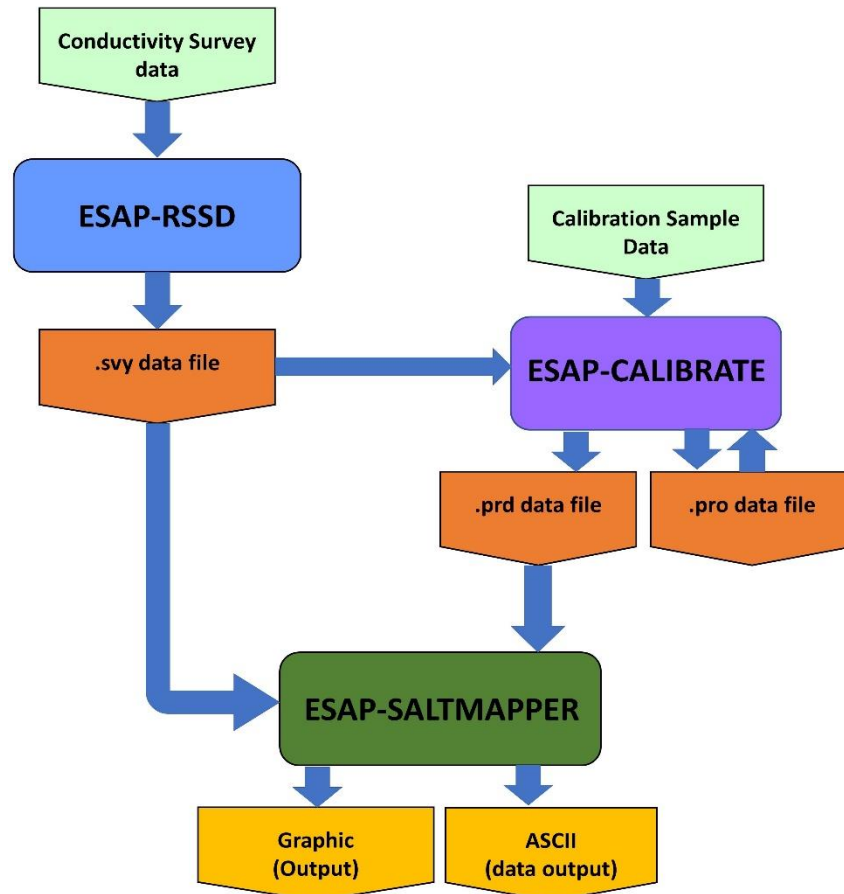


Fig. 2.6: ESAP-95 software bundle: Program flowchart

2.3.1.2 Soil sampling

Six locations covering the full range of EM38 measurements and the entire study area were chosen with the ESAP-Response Surface Sampling Design (ESAP-RSSD) software (Lesch *et al.*, 2002) for soil sampling and EM38 calibration purposes (Fig. 2.5). This software uses the «response surface sampling design» statistical methodology to select a set of sample sites that optimizes the prediction model (Lesch *et al.*, 2002a). The automatic selection of calibration sites saves time and work for the researcher and optimizes the calibration model. The obtained sampling design had an optimization criteria value of 1.03, indicating an excellent uniformity (evenly spread across the field) of our sampling plan, according to Lesch *et al.* (2000)

2.3.1.3 Mapping of EC_a and EC_e

After processing the data in ESAP software, the EC_a data, as well as the predicted EC_e data, were plotted using SaltMapper (Lesch *et al.*, 2002) and ArcGIS 10.5.

2.3.2 Soil texture and dry bulk density

Soil samples down to 80 cm depth (0-20, 20-40, 40-60, and 60-80 cm) were collected from 15 randomly selected locations in each of the two fields. Thus, 60 soil samples were collected from each of the fields and analyzed for soil texture using the Hydrometer method (Bouyoucos, 1936) at Soil and Water Lab, USPCAS-W, MUET Jamshoro. Based on the resulting soil texture, interpolated soil texture GIS maps of all three depths for both fields were prepared using ArcGIS 10.5.

2.3.3 Soil moisture measurement

The soil moisture down to 80 cm depth (at the intervals of 0-20, 20-40, 40-60 and 60-80 cm) was determined at regular time intervals using the gravimetric method. For this, soil samples were collected from four randomly selected locations from each of the salinity level, i.e., low ($EC < 3$ dS/m), medium ($EC = 3-5$ dS/m) and high ($EC > 5$ dS/m) at regular intervals after 2, 10, and 15 days of irrigation. Thus, 48 samples were collected each time from all 12 locations, as shown in Fig. 2.7. The samples were initially weighed and then oven-dried and reweighed for determining the gravimetric moisture content using the relation 3.1.

$$\text{Moisture Content } (\theta_m) = \frac{W_w - W_d}{W_d} \quad (3.1)$$

Where W_w is the weight of wet soil, W_d is the weight of dry soil, and θ_m is gravimetric moisture content. The moisture content on a wet basis (θ_m) was also converted to moisture content on volume (θ_v) basis by multiplying θ_m with the bulk density of soil using relation 3.2.

$$\theta_v = \frac{\rho_d}{\rho_w} \theta_m \quad (3.2)$$

Where ρ_d is dry density of soil and ρ_w is the density of water.

Undisturbed soil samples using soil cores were also collected for determining the dry bulk density of the soil. These samples were dried and weighed. The dry density of soil samples was determined using relation 3.3.

$$\rho_d = \frac{W_d}{V} \quad (3.3)$$

Where V is the volume of the soil core.



Fig. 2.7: Soil sampling locations for moisture content determinations

2.3.4 Monitoring of groundwater table depth

The groundwater depth was measured weekly from the piezometers installed at both the fields under the project using water level sounder. The water depth data thus obtained was then plotted against the date of the reading to monitor the fluctuations in the groundwater

2.3.5 Image classification

Remotely sensed satellite data were used in the land salinity classification through the “training” of the data. The image classification was done through supervised image classification. The maximum likelihood algorithm was used to produce supervised classified salt-affected areas in the field. The whole process of supervised classification is summarized in the flowchart in Fig. 2.8.

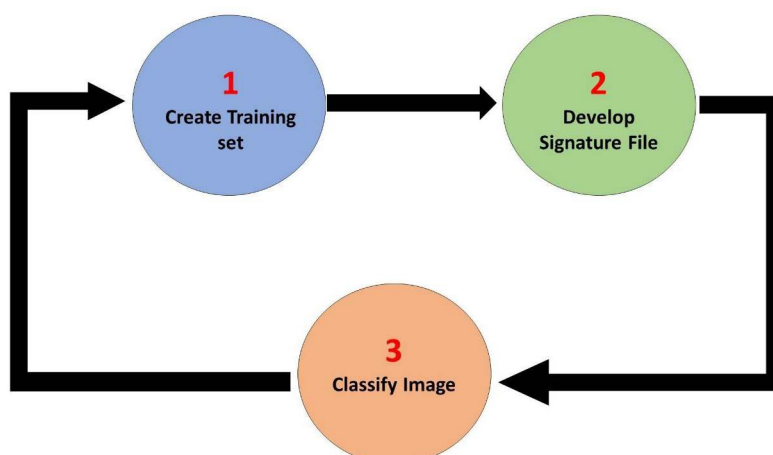


Fig. 2.8: Flow chart of the supervised classification

2.3.6 Climatic data

The daily weather data were obtained from the Drainage and Reclamation Institute of Pakistan (DRIP) Tandojam, which is located at about 41 km away from the Field-I. The climatic data included daily temperature, rainfall, relative humidity, sunshine duration, and wind direction and velocity (Annex A).

2.3.7 Reflectance with a multispectral radiometer (MSR)

The light reflectance from the mustard and cotton crops at locations having low, medium, and high salinity were measured using a multispectral radiometer (MSR), as shown in Fig. 2.9. The MSR reflectance was measured at equal time intervals throughout the growing season. The MSR measured the reflectance in Blue, Green, Red, and NIR bands. For measuring the land surface temperature (LST), a thermal sensor accessory was also attached to MSR. For each location, three MSR readings were taken from three different positions avoiding any shadow over the place. The average of all three readings was taken as the reflectance of that particular place



Fig. 2.9: Measuring the light reflectance through MSR

2.4 Remote Sensing (RS) for Actual Crop Water Use

The effects of soil salinity on crops were mapped based on a combination of multi-level multispectral ground- and space-borne remotely-sensed data using spatially

distributed ET_a estimation algorithms (Gowda *et al.*, 2008) or with salinity stress algorithms (Hamzeh *et al.*, 2016). The high, medium, and low salinity locations were selected based on their detected soil salinity concentration. At those locations, soil water content (SWC) at four depths, i.e., 0-20, 20-40, 40-60 and 60-80 cm) was continuously measured manually at regular intervals (section 2.3.3) to determine variations in soil water status. The derived volumetric soil water content, on an hourly basis, was used in a soil water balance (SWB) method to calculate the crop actual water use or ET_a . Also, water table levels (fluctuations and depths from the surface), rainfall amount, and near-surface reference ET estimate were measured.

2.4.1 Crop phenology and yield

Crop phenology, canopy height, percent cover, and leaf area index at the monitoring locations were also recorded regularly to quantify impacts of salinity on crop growth throughout the growing season. Crop yield (dry mass) also was measured at the end of the growing season by harvesting a sub-sample of plants (e.g., all plants within 1 m² area) at each sampling site. The harvested parts (e.g., grains) were dried in an oven at 70°C until constant mass. Crop yield was used to correlate seasonal ET_a and salinity concentration to effects on crop production.

2.4.2 ET_a and soil salinity

Seasonal ET_a and vegetation indices maps were coupled with ground-based samples of soil salt concentrations and electromagnetic induction based salt maps to develop a relationship to calibrate a model for quantifying spatially, soil salinity levels and effects of salinity on crops, and thus develop crop production functions drawn from these relationships. The methodology for each site is illustrated in Fig. 2.9. Validation of the resulting maps was performed using soil water content (SWC) based ET_a data and the calibrated EM-38 EC maps, crop biophysical data, and crop yield data. The statistical analysis used to determine the model(s) performance included the coefficient of determination (R^2) for regressions, mean bias error (MBE), and root mean square error (RMSE).

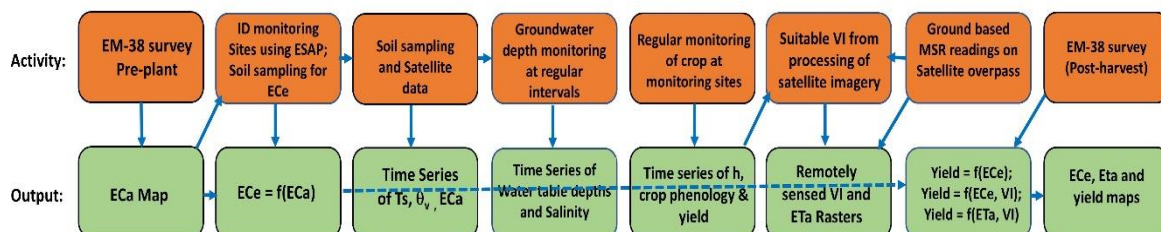


Fig. 2.10: Methodology flow diagram.

The dashed arrow indicates that data and relationships will be aggregated to develop the yield and ET_a functions.

[ECa = apparent bulk electrical conductivity (EC); ECe = EC of soil extract; ET_a = actual crop evapotranspiration; $f()$ = function of; h = height of crop; ID = identify; LAI = leaf area index; MSR = multispectral radiometer; Ts = soil temperature; VI = vegetation index; θ_v = volumetric soil water content]

3. RESULTS AND DISCUSSIONS

3.1 Soil Texture

Spatial distribution of soil texture at 0-20, 20-40, 40-60, and 60-80 cm soil depths (Fig. 3.1) at Deshak Agricultural Farm (Experimental Field-I) reflected that in the top 20 cm layer silty clay loam was the dominant soil texture followed by clay soil. While in the underlying soil layers, silty clay loam and silty clay were the dominant soil textural classes. No significant spatial trend in soil texture was observed.

In the case of the Aamir Agricultural Farm (Experimental Field-II), clay was the dominant soil texture followed by clay loam soil in the top 20 cm layer. While in the underlying soil layers, clay loam (20-40 cm), silty clay (40-60 cm), and clay loam (60-80 cm) were the dominant soil textural classes. No significant spatial trend in soil texture was observed.

3.2 Moisture Content

The spatial distribution of soil moisture in the 0-20 cm soil depth after (a) two days, (b) ten days, and (c) 15 days after irrigation at Deshak Agricultural Farm (Experimental Field-I) is presented in 2D and 3-D view in Fig. 3.3. It reflects that after two days of irrigation, the moisture content in the soil ranged between 32 and 37% while it gradually decreased to 19 to 24% after ten days and 14 to 18% after 15 days of irrigation. It depicts that there was enough moisture in the top 20 cm soil to support the

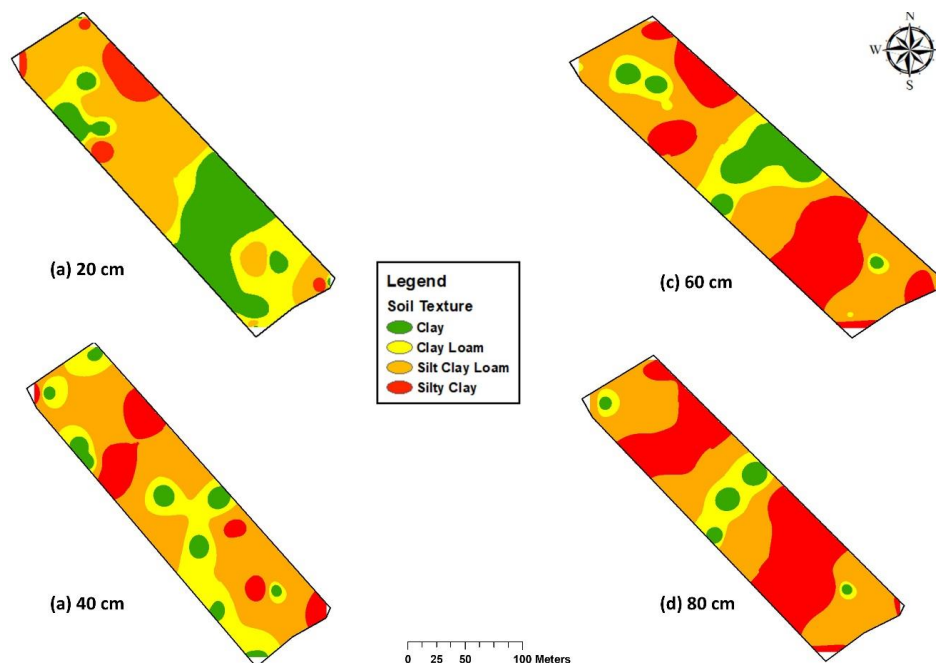


Fig. 3.1: Spatial distribution of soil texture at (a) 0-20 cm, (b) 20-40 cm, (c) 40-60 cm, and (d) 60-80 cm soil depths at Deshak Agricultural Farm (Experimental Field-I)

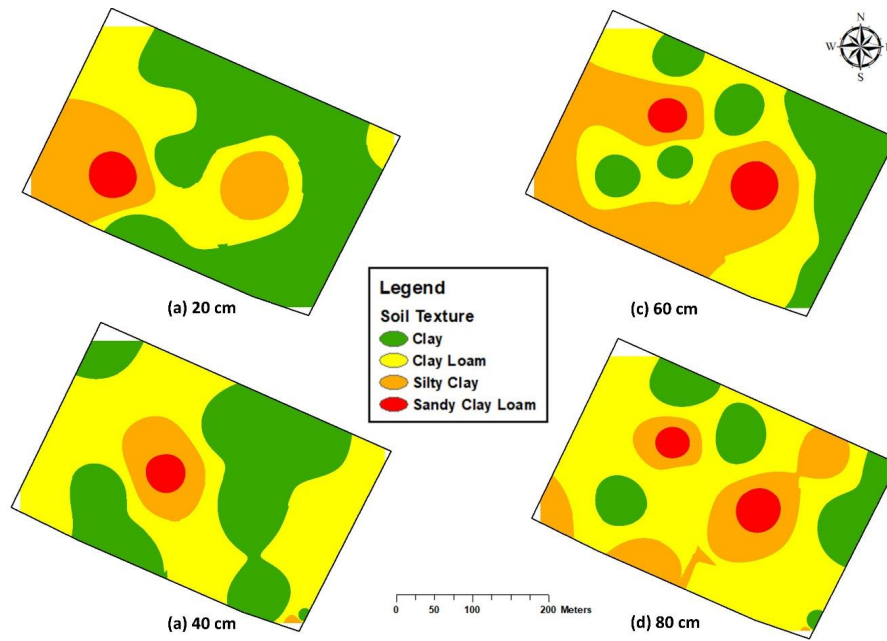


Fig. 3.2: Spatial distribution of soil texture at (a) 0-20 cm, (b) 20-40 cm, (c) 40-60 cm, and (d) 60-80 cm soil depths at Aamir Agricultural Farm (Experimental Field-II)

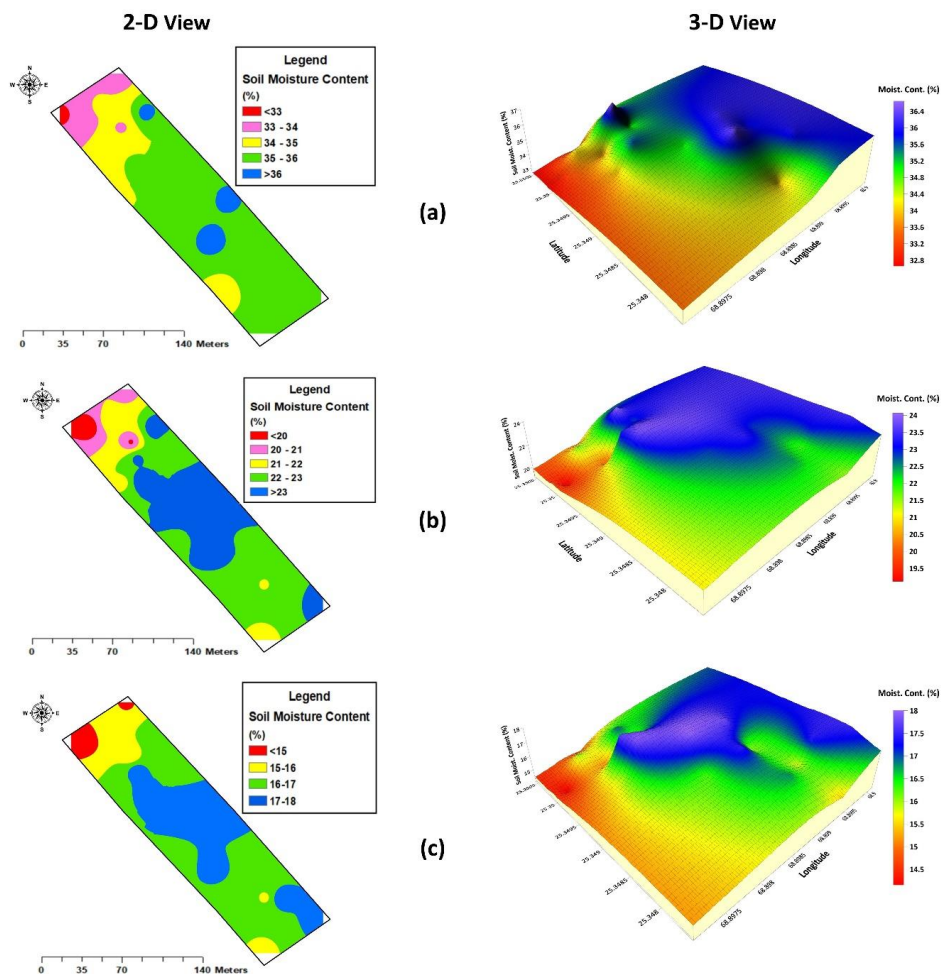


Fig. 3.3: 2-D and 3-D view of the spatial distribution of soil moisture in 0-20 cm soil depth after (a) 2 days (b) 10 days, and (c) 15 days after irrigation at Deshak Agricultural Farm (Experimental Field-I)

plant growth even after 15 days of irrigation. North-Western side of the land retained less water compared to the rest of the field, which might be due to the impact of soil organic matter and soil porosity.

Fig. 3.4 shows the spatial distribution of soil moisture in the 0-20 cm soil depth after (a) two days, (b) ten days, and (c) 15 days of irrigation at Aamir Agricultural Farm (Experimental Field-II) is presented in 2D and 3-D view. It reflects that after two days of irrigation, the moisture content in the soil ranged between 31 and 35% while it gradually decreased to 16 to 19% after ten days and 12 to 15% after 15 days of irrigation. It depicts that there was enough moisture in the top 20 cm soil depth to support the plant growth even after 15 days of irrigation. No significant spatial trend in variation of soil moisture was observed

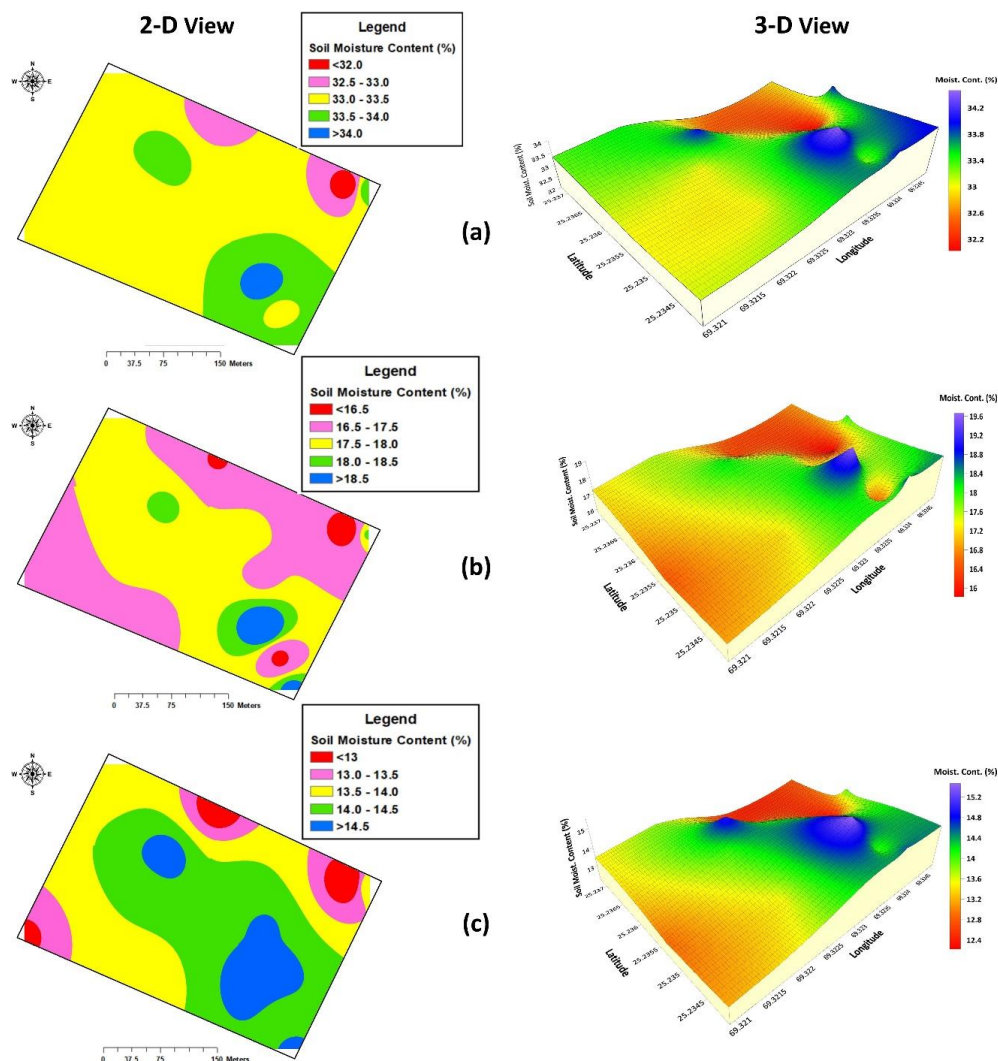


Fig. 3.4: 2-D and 3-D view of the spatial distribution of soil moisture after (a) 2 days (b) 10 days, and (c) 15 days of irrigation at 0-20 cm soil depth at Aamir Agricultural Farm (Experimental Field-II)

3.3 Soil Salinity

3.3.1 Experimental field-I

Apparent electrical conductivity (EC_a) in a soil layer of 0.75 m obtained through EMI survey using EM38-MK2 and plotted using ESAP SaltMapper 3.5 and Surfer 16 software (Fig. 3.5). The plots show that the EC_a ranges from <4.66 to >5.23 dS/m. The EC_a was higher along the edge of the eastern side of the field, while central areas had low EC_a.

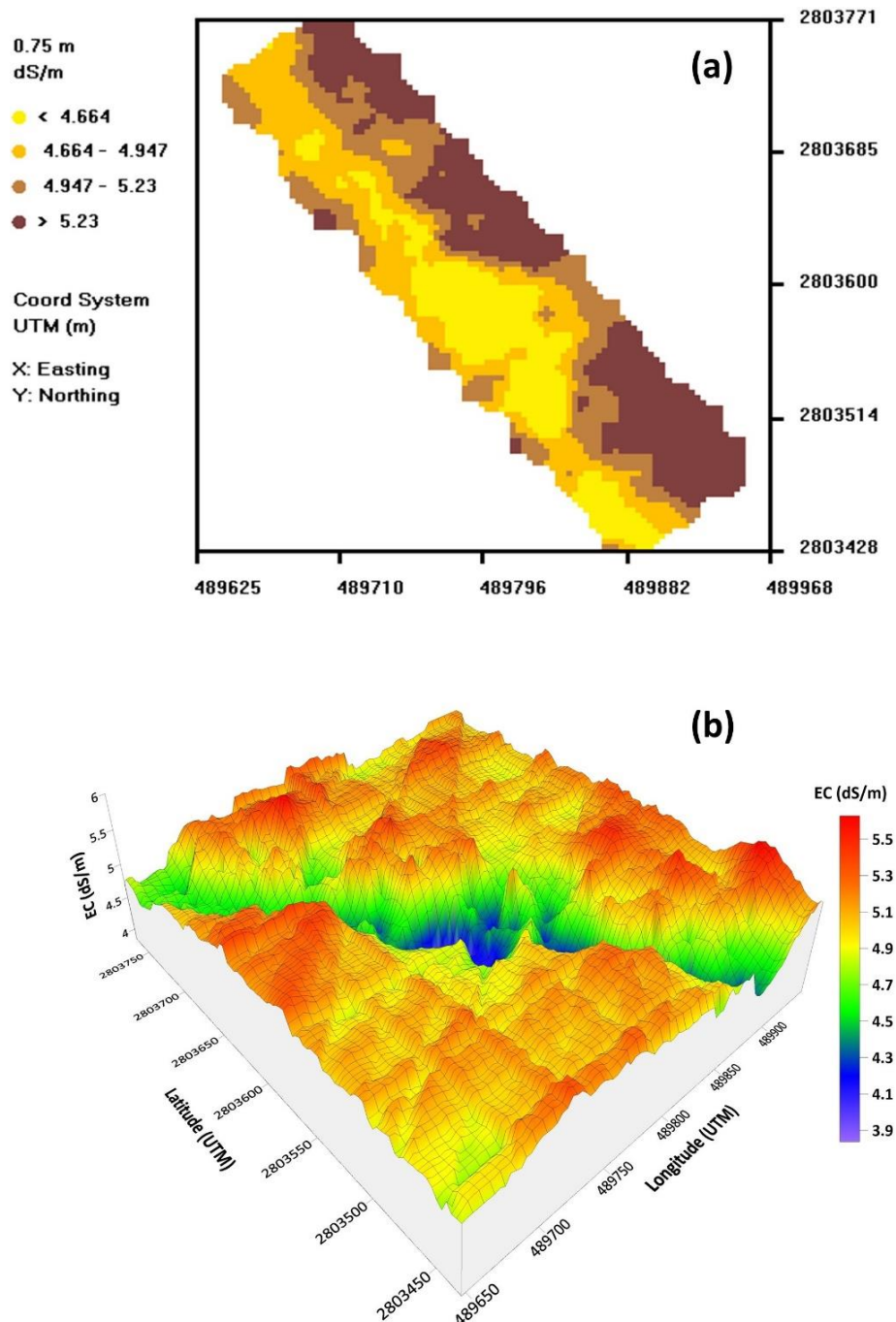


Fig. 3.5: Spatial distribution of apparent electrical conductivity (EC_a) of 0.75 m layer of Deshak Agricultural Farm (Experimental Field-I) obtained through EMI survey and plotted using (a) SaltMapper and (b) Surfer 16

Similarly, the ECa values recorded for the soil layer down to 1.5 m showed that it ranges from < 4.4 to >5.0 dS/m (Fig. 3.6). A similar pattern of ECa was observed for the 1.5 m soil depth as that of 0.75 m soil depth.

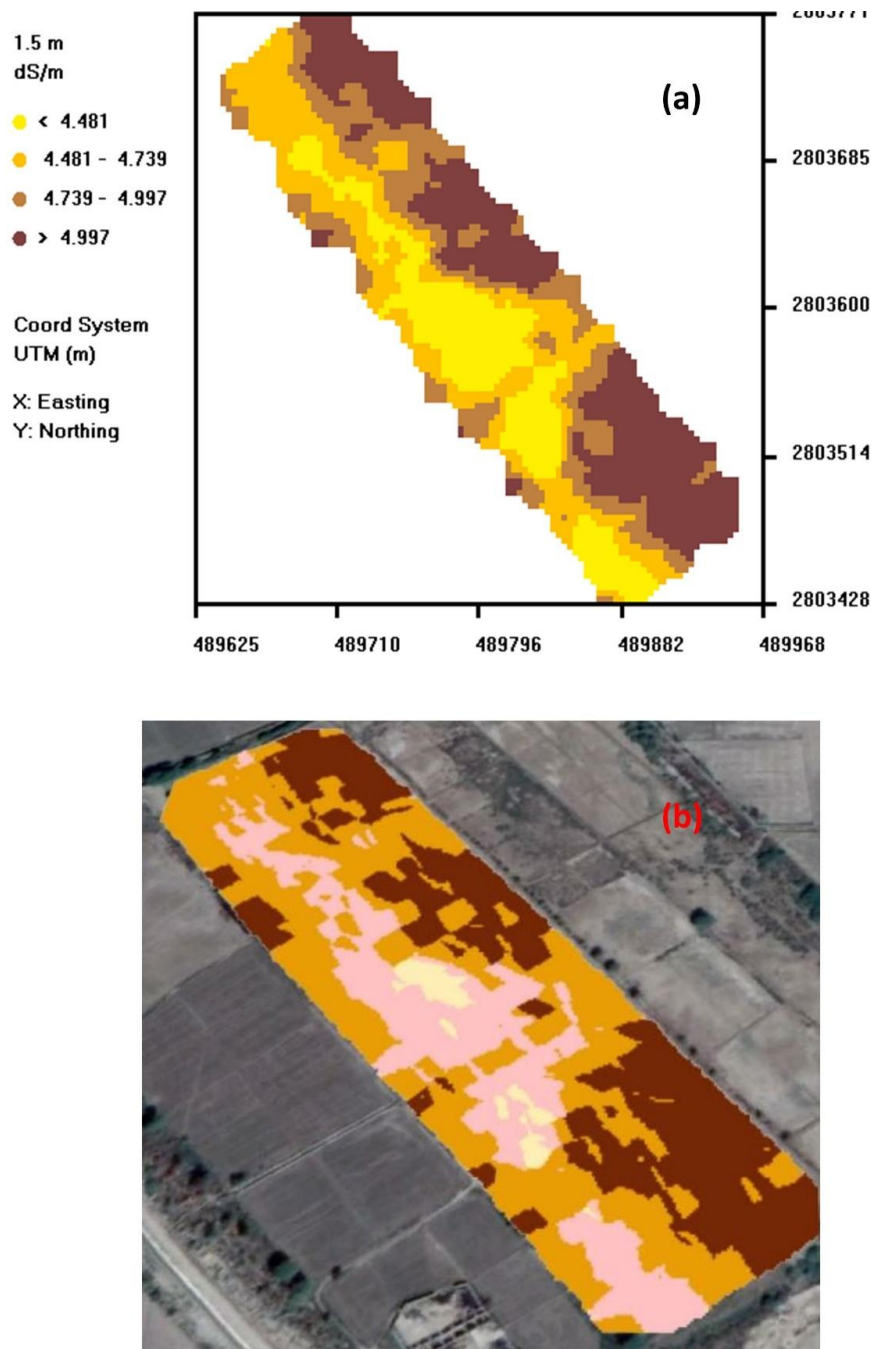


Fig. 3.6: Spatial distribution of apparent electrical conductivity (EC_a) of 1.5 m soil layer of Deshak Agricultural Farm (Experimental Field-I) obtained through EMI survey and plotted using (a) SaltMapper 3.5 and (b) ArcGIS 10.5

The average electrical conductivity of the soil saturation extract (EC_e) of 0.8 m soil layer predicted from the ESAP-Calibrate 3.5 and plotted using SaltMapper 3.5 is plotted in Fig 3.7. The predicted EC_e values are based on the EC_e of the soil samples collected from the locations obtained with ESAP-RSSD 3.5 software. The data shows that the EC_e values are slightly higher than EC_a . It might be due to the soil moisture

content of the soil down to 1.5 m depth was less than the field capacity during EMI surveys as also reported by Hanson and Kaita (1997), Bennett *et al.* (2000), Turnham (2003) and Wittler *et al.* (2006) who found substantial changes in the EC_a readings as soil-water content changed.

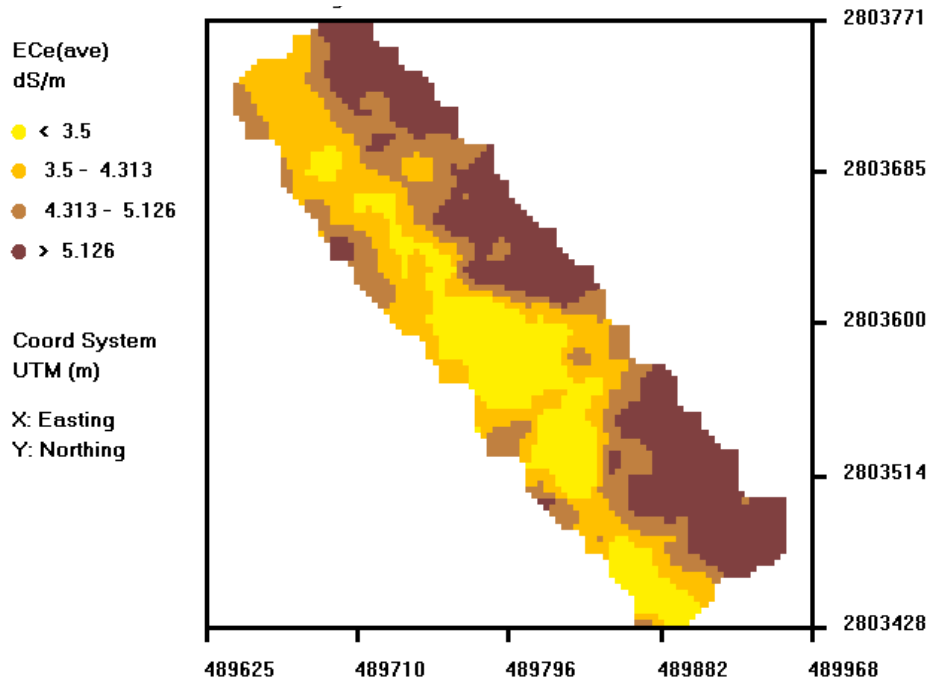


Fig. 3.7: Spatial distribution of predicted electrical conductivity of soil saturated extract (EC_e) of 0.8 m soil layer of Deshak Agricultural Farm (Experimental Field-I) predicted from ESAP-Calibrate 3.5 and plotted using SaltMapper 3.5

3.3.1.1 Relationship between EC_a and EC_e

The apparent soil electrical conductivity (EC_a) was plotted against the electrical conductivity of the soil saturation extract (EC_e), as shown in Fig. 3.8. It reflects that the EC_a values are slightly smaller than the EC_e values, which might be due to the impact of soil water content (SWC) being less than the field capacity.

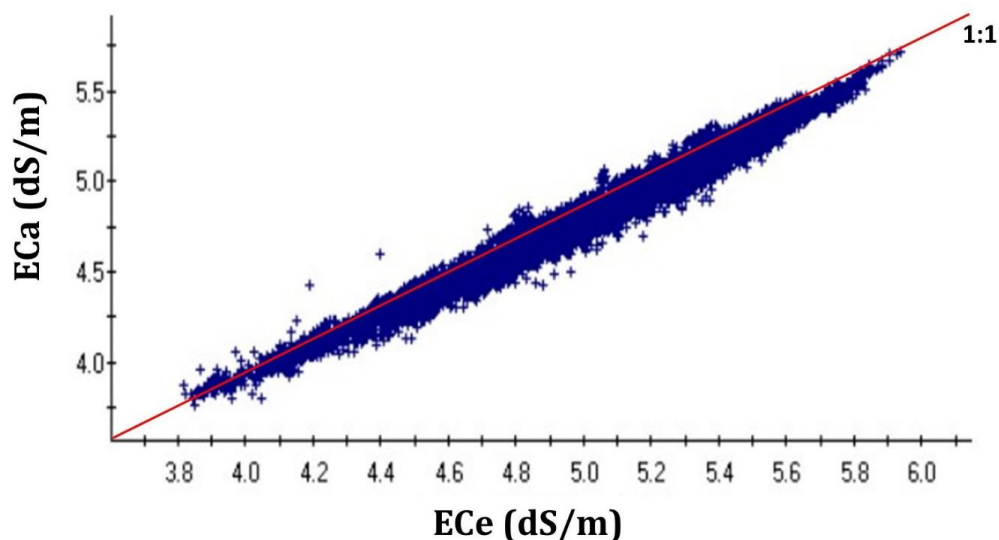


Fig. 3.8: Relationship between EC_a and EC_e

3.3.2 Experimental field-II

Fig. 3.9 shows the ECa in a soil layer of 0.75 m obtained through EMI survey using EM38-MK2 and plotted using ESAP SaltMapper 3.5 and Surfer 16 software. The plots show that the ECa ranged from 2.8 to >5.5 dS/m. The plots depict that the ECa was higher along the edge of the eastern side as well as at a small portion of the central area of the field. While the rest of the field had a low ECa.

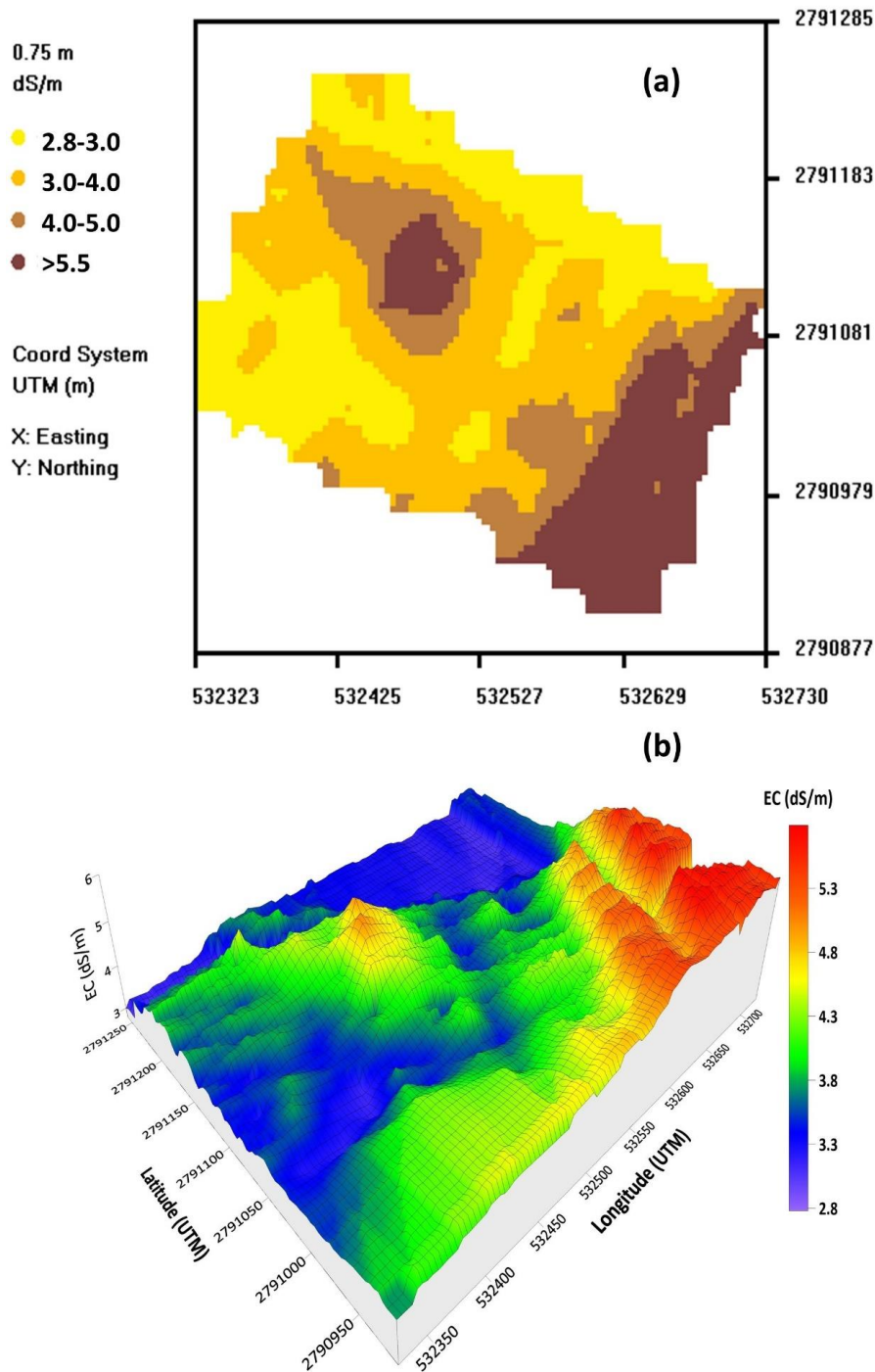


Fig. 3.9: Spatial distribution of apparent electrical conductivity (EC_a) of 0.75 m layer of Aamir Agricultural Farm (Experimental Field-II) obtained through EMI survey and plotted using (a) SaltMapper and (b) Surfer 16

The ECa data were also obtained for a soil layer of 1.5 m through EMI survey using EM38-MK2 and plotted using ESAP SaltMapper 3.5. Fig. 3.10 shows that the ECa ranges from <3.6 to >4.50 dS/m. It was noted that ECa values of 1.5 m soil layer followed the same pattern as that of 0.75 m soil layer, but the ECa at the lower layer was less than that of the upper layer. It might be due to solute transport from the bottom soil layer to the top layer during evaporation

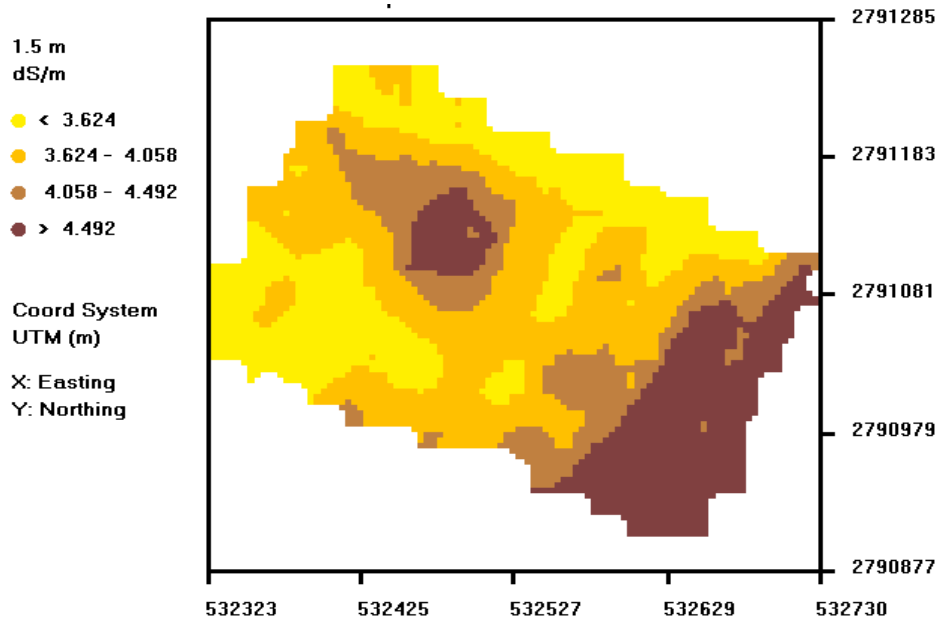


Fig. 3.10: Spatial distribution of apparent electrical conductivity (EC_a) of 1.5 m soil layer of Aamir Agricultural Farm (Experimental Field-II) obtained through EMI survey and plotted using SaltMapper 3.5

3.4. Water Table and Irrigation

3.4.1 Irrigation

The water applied during each irrigation was measured by installing cut-throat flume in the watercourse. The volume of water per irrigation, thus determined, was divided with the area of the field to get the amount of irrigation water in terms of depth. The depth of irrigation water applied per irrigation to mustard crop against the dates of irrigation is plotted in the graph shown in Fig. 3.11. The total depth of water applied to Rabi crop (mustard) was 411.65 mm, including 27.1 mm of rainwater.

Similarly, the depth of irrigation water applied to cotton crop per irrigation is plotted against the dates of irrigation, as shown in Fig. 3.12. The total depth of water applied to cotton crop 953.9 mm, including 264 mm of rainfall. The normal crop water requirement of the cotton crop is 880 mm. The higher crop water consumption is due to unexpected rainfall.

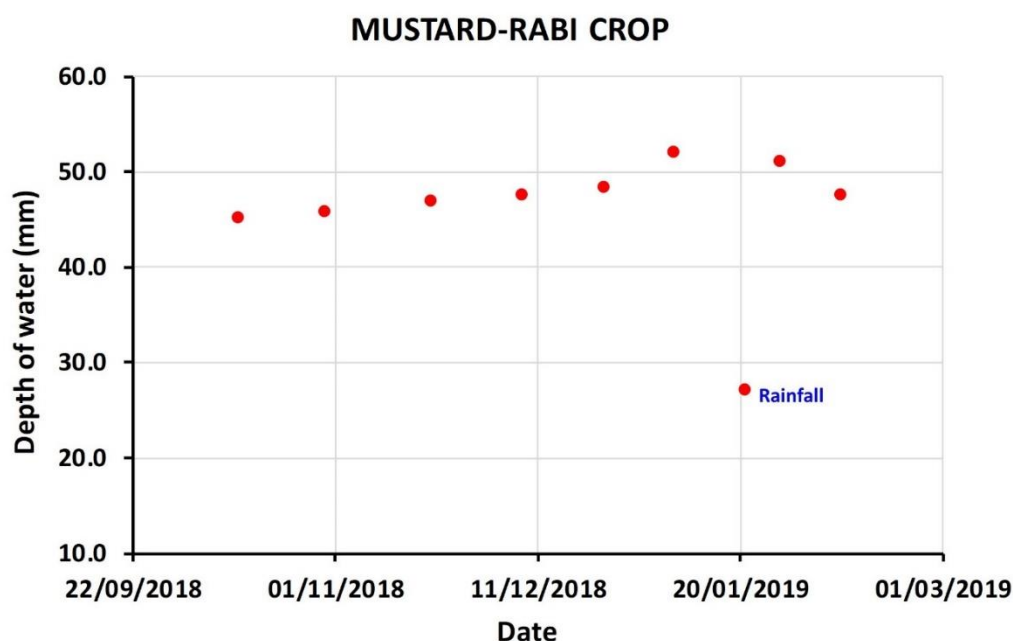


Fig. 3.11: Depth of rainfall and irrigation water applied to the mustard crop at Experimental Field-I

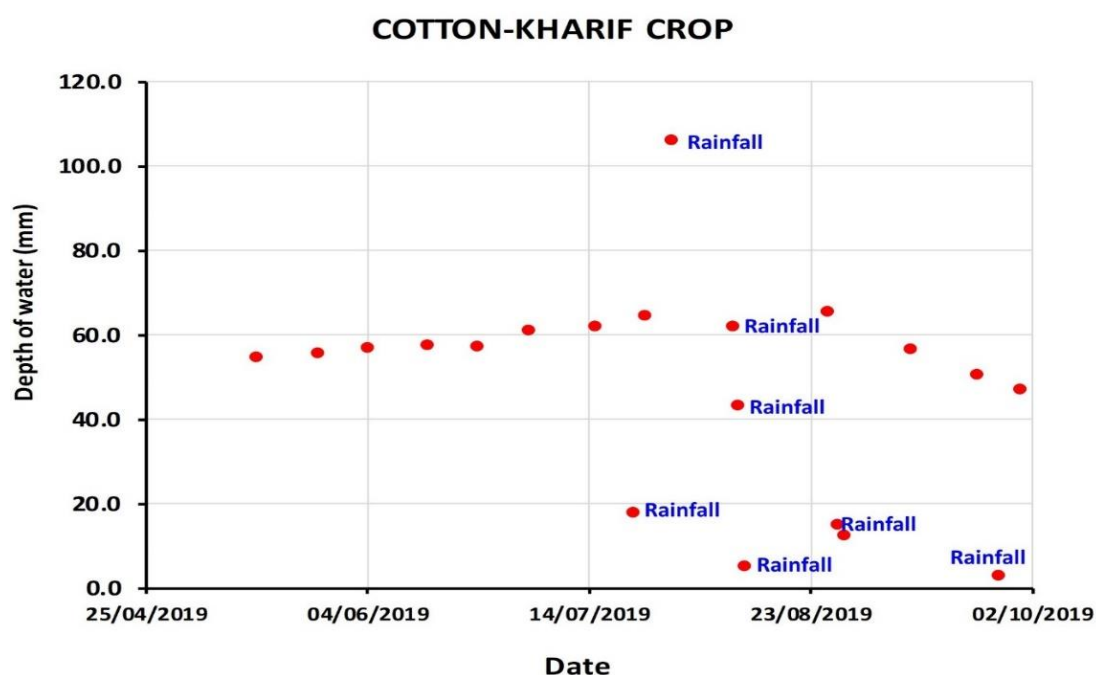


Fig. 3.12: Depth of rainfall and irrigation water applied to the cotton crop at the Experimental Field-I

The depth of irrigation water applied per irrigation to mustard crop at Field-II against the dates of irrigation is plotted in the graph shown in Fig. 3.13. The total depth of water applied to Rabi crop (mustard) was 384.4 mm.

Similarly, the depth of irrigation water applied to cotton crop per irrigation is plotted against the dates of irrigation, as shown in Fig. 3.14. The total depth of water applied to cotton crop 970 mm, including 130 mm of rainfall. The higher crop water consumption is due to over application of water due to unexpected monsoon rainfall.

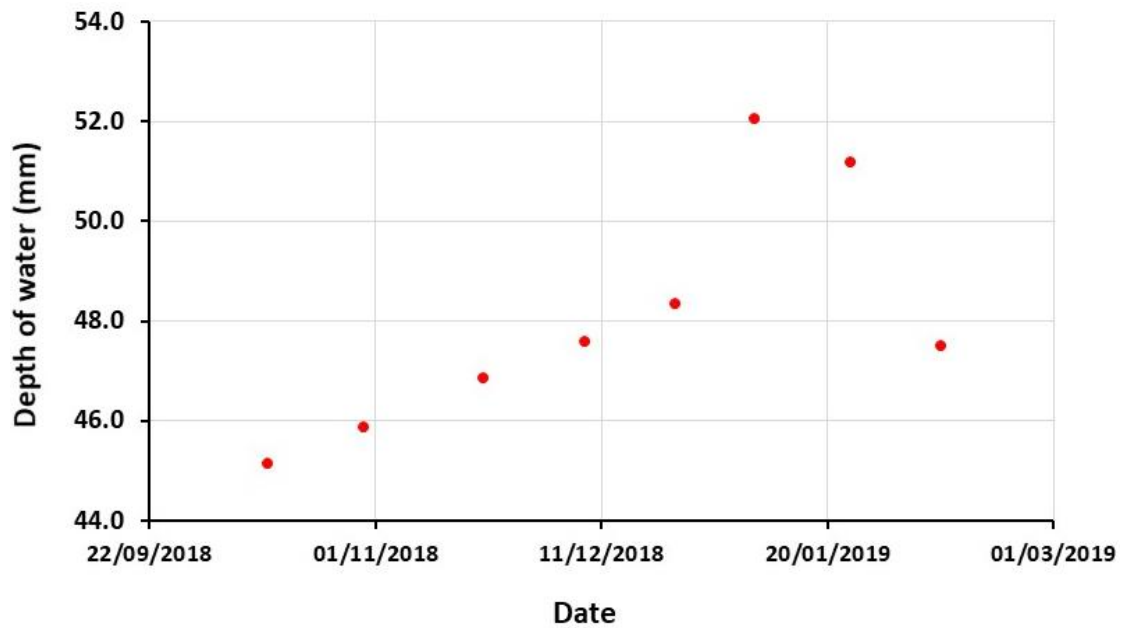


Fig. 3.13: Depth of irrigation water applied to the mustard crop at Experimental Field-II

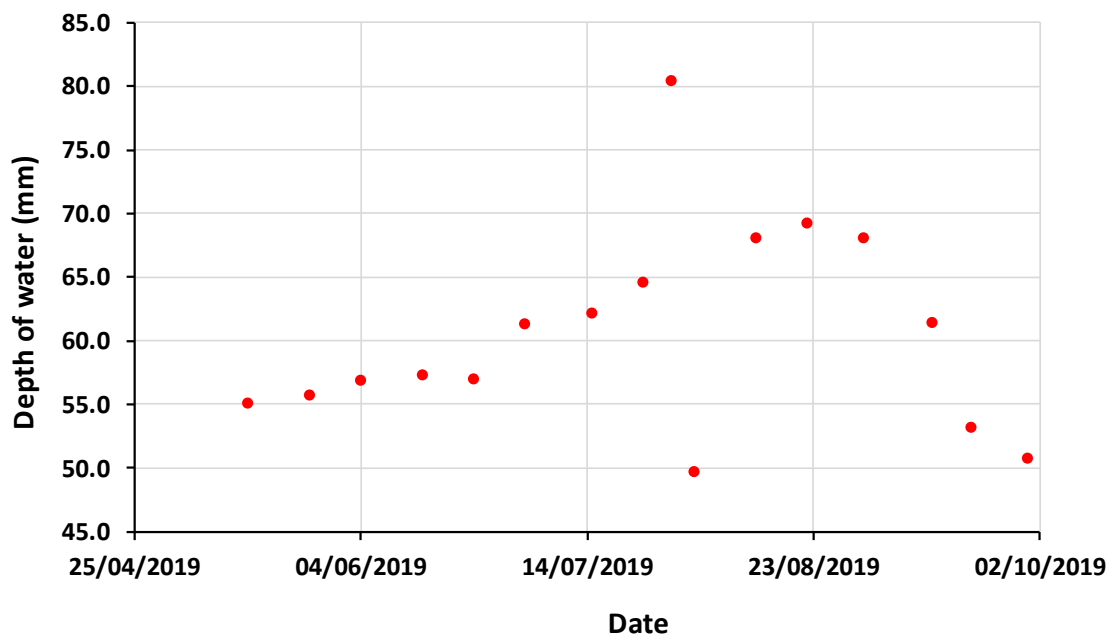


Fig. 3.14: Depth of irrigation water applied to the cotton crop at Experimental Field-II

3.4.2 Water table

The groundwater table fluctuations were recorded through the piezometers installed at the corners of the field, about 300 m apart. Fig. 3.15 depicts that the water table depth fluctuated between 3.75 and 4.6 m. The maximum drop in the water table was observed from September to November and May to June. While the water table was higher during December, July, and August.

The groundwater table fluctuations at the Experimental Field-II shows that the water table fluctuated between 1.75 and 2.4 m depths (Fig. 3.16). The maximum drop in the

water table was observed from March to July, while the water table was higher during August and September.

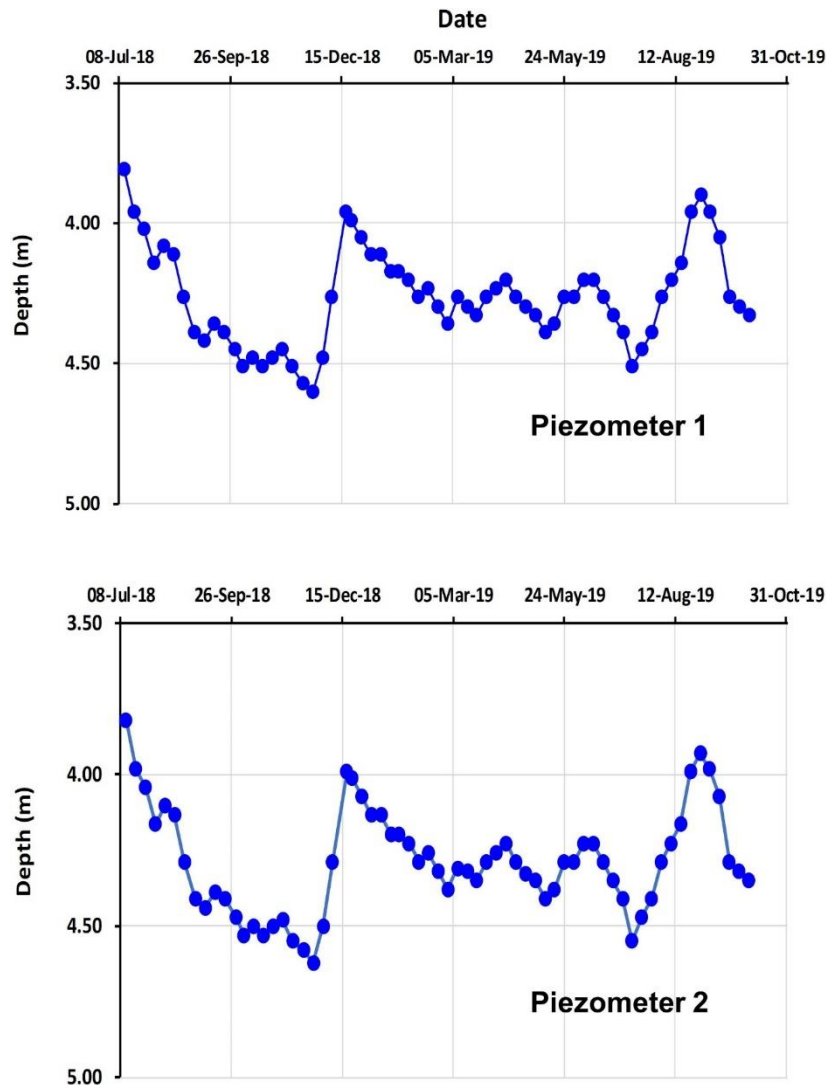


Fig. 3.15: Temporal fluctuation in the water table depth at the Experimental Field-I

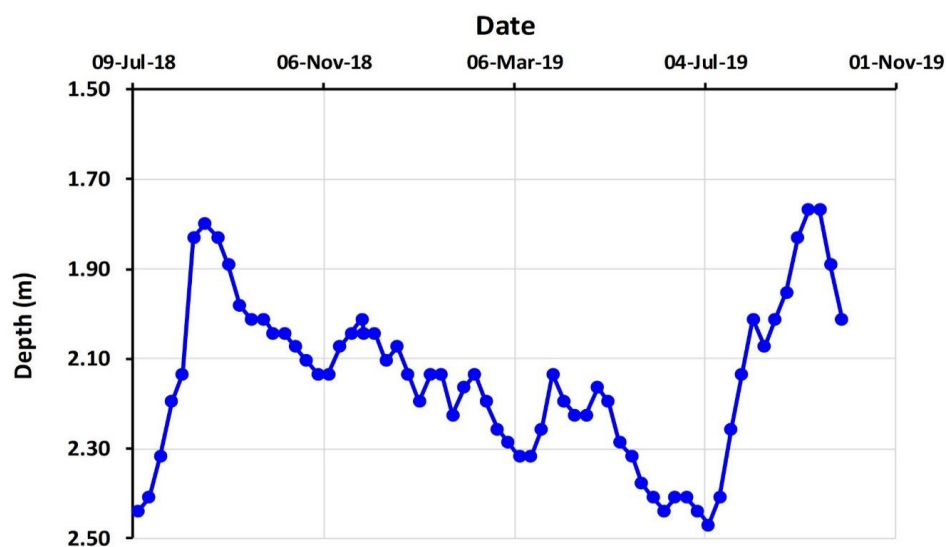


Fig. 3.16: Temporal fluctuation in the water table depth at the Experimental Field-II

3.5 Vegetation Indices

Fig. 3.17 shows the plots of spatial and temporal variation of NDVI of mustard crop grown at Experimental Field-I. It reflects that during the initial crop growth period, the NDVI of most of the field was very low, especially for the south-eastern part of the field. While the NDVI ranged between 0.17 and 0.59 during the peak growth of the crop in mid-December, 2018. Later on, in January 2019, it started to decrease. The NDVI for areas with high salinity always remained low in the range of 0.05 to 0.30.

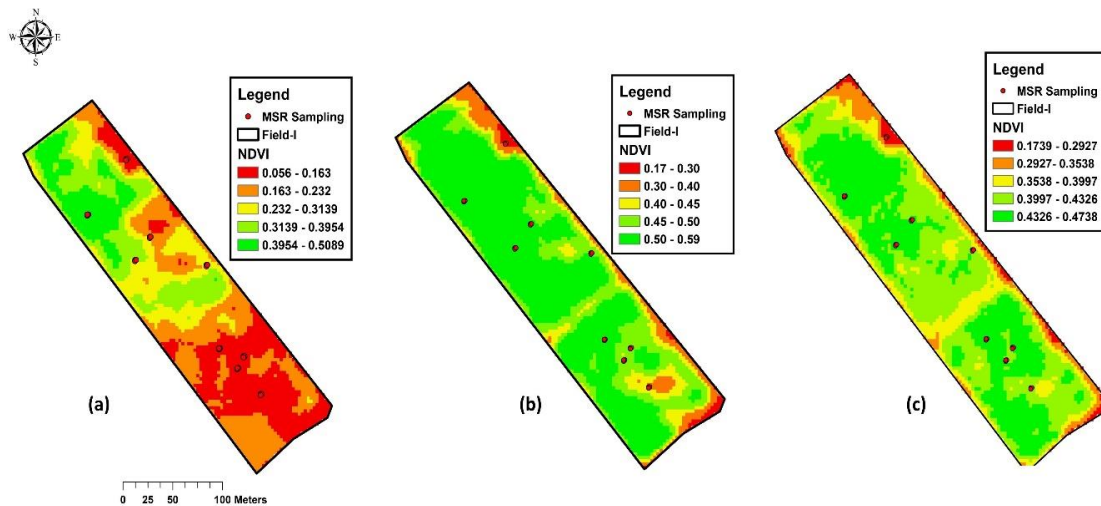


Fig. 3.17: Temporal and spatial variation in the NDVI for the mustard crop at Experimental Field-I (a) Nov. 18, 2018 (b) Dec. 18, 2018 (c) Jan. 18, 2019.

For getting a clear picture of the NDVI of areas with varying degrees of soil salinity, the NDVI of the low, medium, and high salinity areas at different crop growth stages are plotted in Fig. 3.18. It suggests that NDVI was always high for all three locations with low salinity, whereas locations with high soil salinity had lower NDVI throughout the crop growth period. The green pigment in the plant leaves reflects light relatively higher in the NIR band, thus causes higher NDVI value as also reported by Knipling (1970), Badgely *et al.* (2017), Drisya *et al.* (2018).

The temporal variation in NDVI of locations with low, medium, and high salinity is presented in Fig. 3.19. It depicts that NDVI is lower at the early growth stage of mustard crop, reaches its peak during the peak growth period, and then starts declining when the crop approaches to maturity.

3.6 Multispectral Radiometer (MSR) Reflectance

The temporal variation in light reflectance of the mustard crop from locations with low ($EC < 2$ dS/m), medium (EC 2-5 dS/m) and high salinity ($EC > 5$ dS/m) levels are plotted in Fig. 3.20. The reflectance was measured using MSR. The data shows that reflectance in near infra-red (NIR) band increases from 21% at the initial crop growth stage on

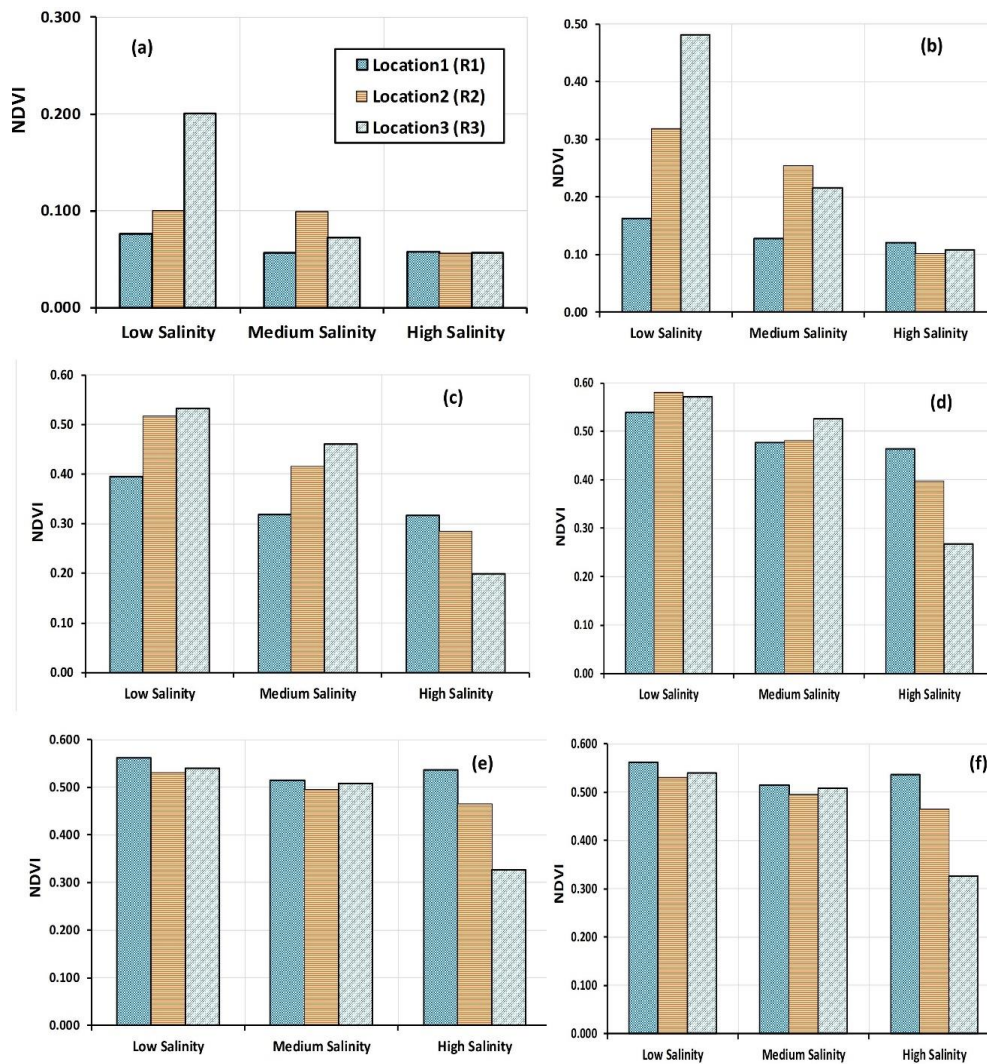


Fig. 3.18: Temporal variation in NDVI for the mustard crop at Experimental Field-I (a) Nov. 03, 2018 (b) Nov. 18, 2018 (c) Dec. 05, 2018 (d) Dec. 18, 2018 (e) Jan. 3, 2019 and (f) Jan. 18, 2019

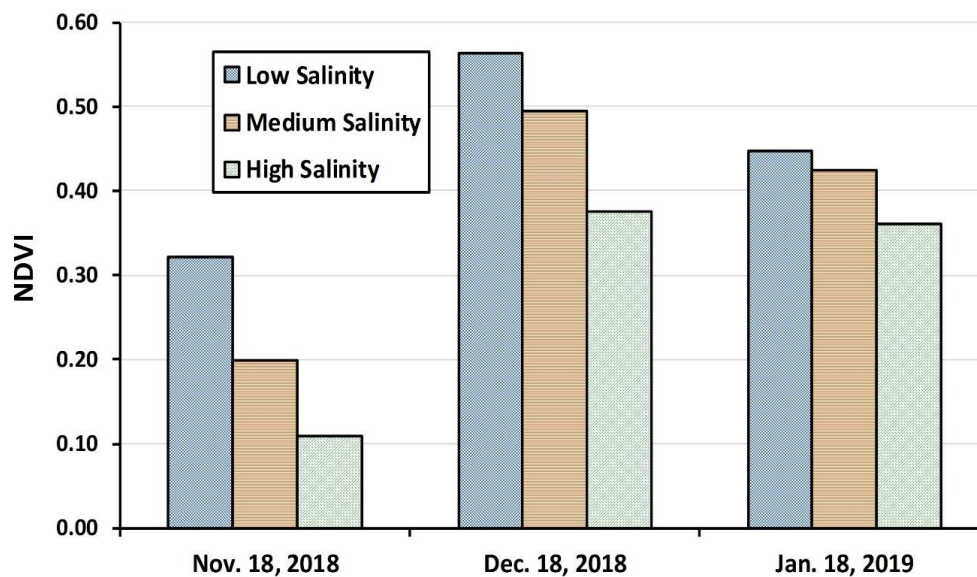


Fig. 3.19: Temporal variation in NDVI for the mustard crop at Experimental Field-I for low, medium and high salinity

November 3 to 40.6% at its peak growth on Dec. 18, 2018, for the locations with low soil salinity. While for the locations with medium and high soil salinity, the reflectance at full growth of crop was 35% and 29%, respectively. Thus, with crop growth, the reflectance in NIR increased, while the reflectance in visible range decreased with the increase in the vegetative cover.

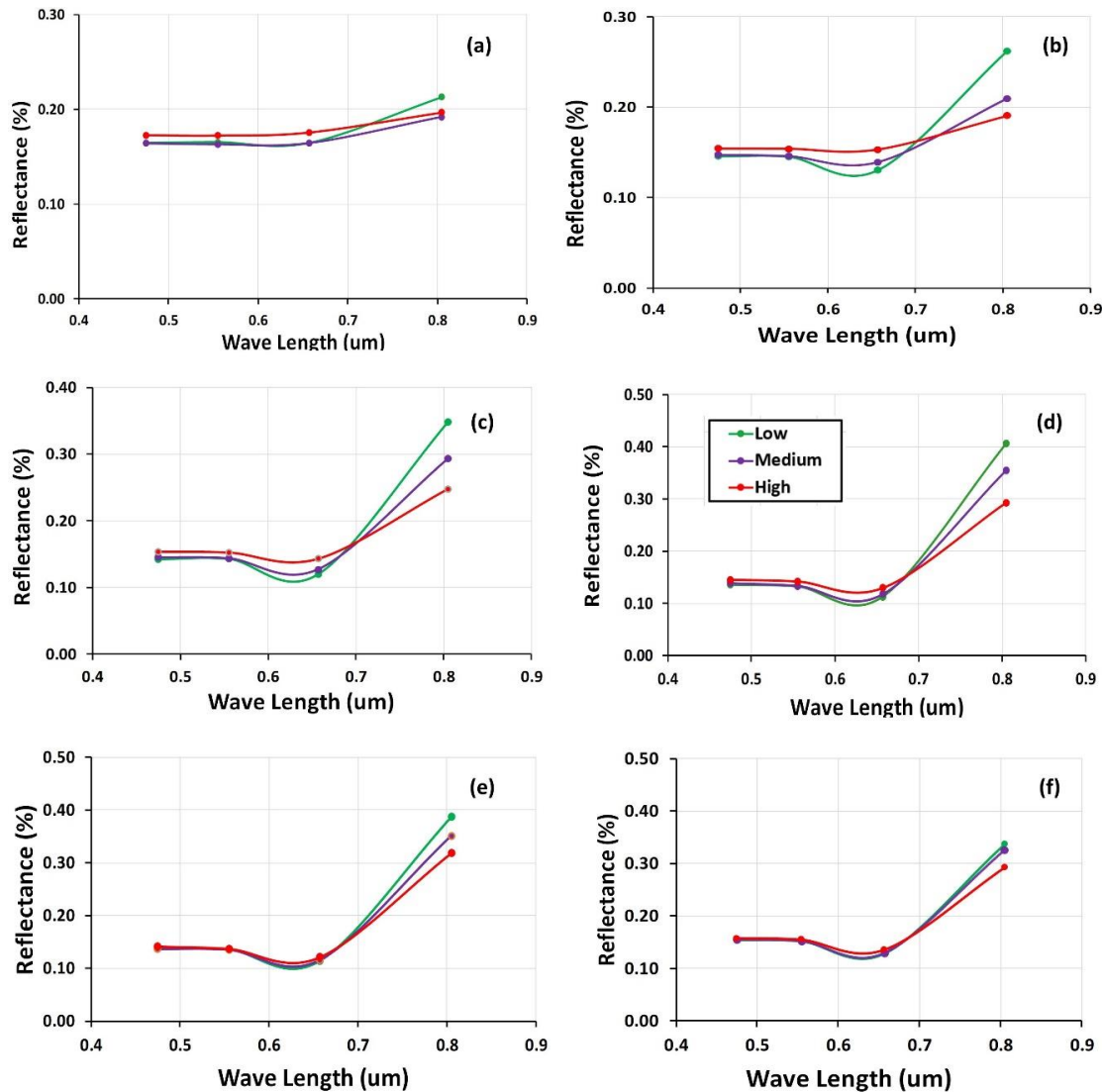


Fig. 3.20: Light reflectance (%) from the mustard field in different bands from the low, medium, and high salinity levels (a) Nov. 03, 2018 (b) Nov. 18, 2018 (c) Dec. 05, 2019 (d) Dec. 18, 2019 (e) Jan. 03, 2019 and (f) Jan. 18, 2019

3.7 Crop Phenology

The root zone salinization is the main problem for plant productivity that is effectively balanced by salt-tolerant halophytic crop. The phenological stages and processes of a plant are usually affected by salinity and field management practices. The cotton crop phenology was observed at different salinity levels:

3.7.1 Plant biomass

Plant biomass observed at low saline area varied from 1066 to 1088 g with an average of 1076 ± 11.1 g. For medium saline areas, it fluctuated between 871 to 1050 g with an average of 958 ± 53.7 g, and in high saline areas, it varied from 408 to 866 g with an average of 721 ± 187.3 g, as shown in Fig 3.21.

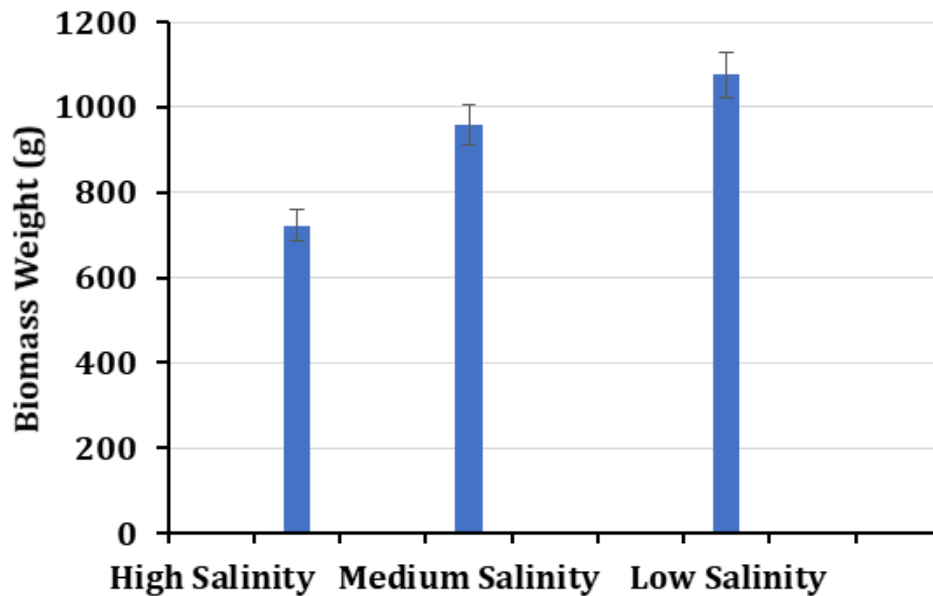


Fig. 3.21: Cotton crop biomass per plant obtained from locations with low, medium and high salinity levels

3.7.2 Plant height

The plant height in low saline areas varied from 135 to 148 cm, with an average of 141 ± 6.5 cm. The height in medium saline areas fluctuated between 121 to 88 cm, with an average of 104 ± 22.6 cm, and in high saline areas, it varied from 66 to 85 cm, with an average of 78 ± 13.4 cm, as shown in Fig. 3.22.

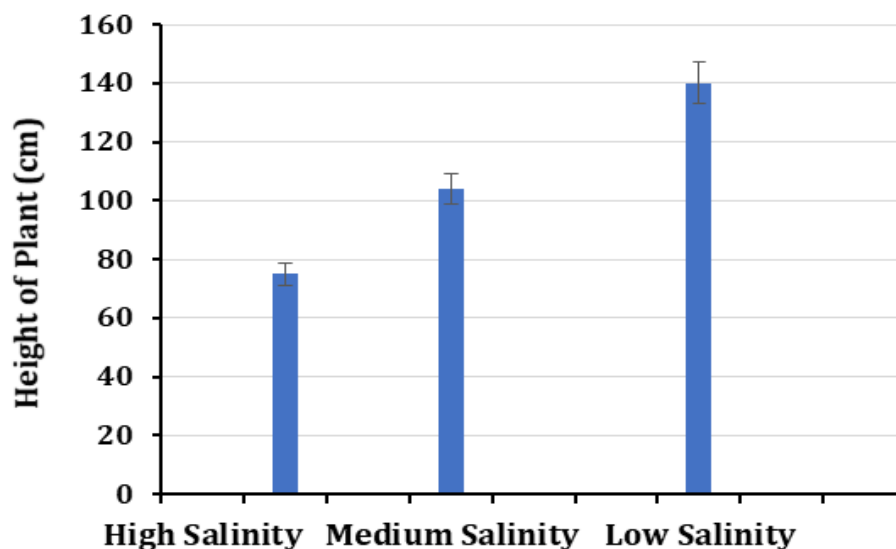


Fig. 3.22: Height of cotton plants grown at locations with low, medium and high salinity levels

3.8 Cotton Yield

3.8.1 Cotton

Yield response of cotton to salinity was observed at different levels of salinity, such as low salinity ($EC < 3 \text{ dS/m}$), medium salinity ($EC \text{ } 3\text{--}5 \text{ dS/m}$), and high salinity ($EC > 5 \text{ dS/m}$). In the low saline area of Field-1, the seed cotton yield varied from 0.39 to 0.42 kg/m^2 with an average of $0.40 \pm 0.015 \text{ kg/m}^2$. Yield values at medium saline soil fluctuated between 0.19 to 0.38 kg/m^2 , with an average of $0.285 \pm 0.05 \text{ kg/m}^2$, and at the high saline area, it varied from 0.06 to 0.17 kg/m^2 , with an average of $0.12 \pm 0.03 \text{ kg/m}^2$, as shown Fig 3.23.

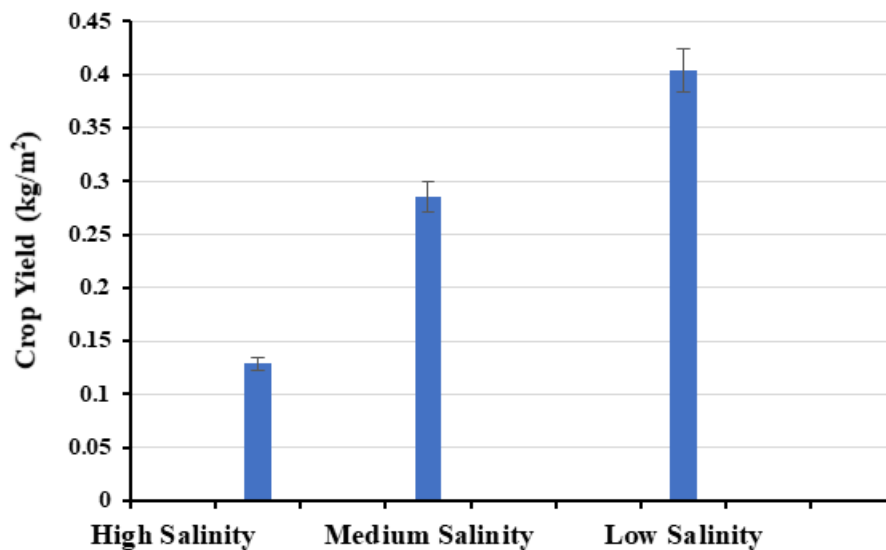


Fig. 3.23: Crop yield obtained from locations with low, medium and high salinity levels

The yield of mustard crop obtained from the selected locations under observations at Experimental Field-I is presented in Table 3.1. It reflects that with increasing soil electrical conductivity (EC_e), the crop yield decreases tremendously such that at medium ($EC = 3\text{--}5 \text{ dS/m}$) and high soil salinity ($EC > 5 \text{ dS/m}$) crop yield decrease by 11.6% and 31.3%, respectively. Similar trend of yield reduction with increase in soil salinity was observed for experimental Field-II for mustard crop. The presence of salts in the soil water matrix decreases the availability of water needed for crop-transpiration due to the impact of osmotic potential. Thus, plants undergo dry water or osmotic stress conditions affecting crop biomass and yield (Oliveira *et al.* 2013; Gupta *et al.*, 2014).

Table 3.1 Mustard crop yield obtained from various locations under observations

Longitude	Latitude	Soil EC	Salinity level	Replications	Yield (kg/pixel)	Mean (kg/pixel)	Yield (kg/ha)	Mean (kg/ha)	Reduction (%)
68.89921	25.348336	EC > 5 dS/m	High Salinity	R1	1.24	1.163	1377.789	1292.603	31.299
68.89944	25.348126			R2	1.15		1277.788		
68.89809	25.350112			R3	1.1		1222.232		
68.89927	25.348445	EC 3-5 dS/m	Medium Salinity	R1	1.45	1.497	1611.124	1662.976	11.614
68.8989	25.349217			R2	1.54		1711.125		
68.89833	25.349455			R3	1.5		1666.68		
68.89903	25.348514	EC < 3 dS/m	Low salinity	R1	1.7	1.693	1888.904	1881.497	0
68.89818	25.349259			R2	1.65		1833.348		
68.89771	25.349634			R3	1.73		1922.238		

3.9 Research Output

3.9.1 M.E. Thesis

1. Nahiyoan, S. A. Soil Salinity Mapping using EM38-MK2 and ESAP software. M.E. Thesis (Under process).

3.9.2 Conference/seminar presentations

1. Siyal, A.A. (2019). Application of EM38-MK2, ESAP, and geospatial tools for determining spatial variation in soil salinity. The paper presented as a keynote speaker in the 1st Two Days International Conference on “Agricultural Engineering and Technologies (ICAET-2019), organized by the Faculty of Agricultural Engineering, Sindh Agriculture University Tandojam, Sindh, Pakistan, Nov. 05-06, 2019.

4. CONCLUSION AND RECOMMENDATIONS

This study was conducted using field, satellite, and multispectral data to quantify the severity of the salinity and its impact on crop yield at two locations in districts Tando Allahyar and Mirpur Khas, Sindh.

4.1 Conclusions

- i. The soil texture of the fields at both the locations was medium to heavy, dominated by silty clay loams and clayey textures.
- ii. The soils at both the locations had enough water holding capacity such that after 15 days after irrigation, the soil had sufficient moisture content to support the crop growth.
- iii. The apparent soil electrical conductivity (EC_a) at the Experimental Field-I ranged from 2.8 dS/m to >8.5 dS/m. While for the Experimental Field-II, the EC_a ranged from 3 dS/m to >7.3 dS/m.
- iv. The correlation plots between EC_a and EC_e (electrical conductivity of saturation extract) showed that EC_a values were slightly lower than the EC_e values, which reflects that EM38-MK2 underestimated soil salinity. It might be due to the impact of soil water content (SWC) being less than the field capacity.
- v. The irrigation water used for mustard and cotton crops was 411.6 mm and 953.9 mm, respectively.
- vi. The continuous monitoring of the groundwater table revealed that the water table depth fluctuated between 3.75 and 4.6 m depths at the Experimental Field-I while it varied between 1.75 and 2.4 m at the Experimental Field-II.
- vii. The NDVI ranged from 0.17 to 0.59 during the peak growth of the mustard crop.
- viii. The NDVI values were always high for low salinity locations, whereas locations with high soil salinity had lower NDVI values throughout the crop growth period.
- ix. The cotton crop yield response to salinity at a low saline area varied from 0.39 to 0.42 kg/m², with an average of 0.40±0.015 kg/m². Yield values at medium saline soil fluctuated between 0.19 to 0.38 kg/m² with an average of 0.285±0.05 kg/m² and at high saline area varied from 0.06 to 0.17 kg/m² with an average of 0.12±0.03 kg/m².
- x. The increased salt concentration in soil decreases the availability of water to the crops.
- xi. NDVI can be used to represent the soil salinity in the area as higher the soil salinity lower the NDVI.

4.2 Recommendations

Based on the present study, it is recommended that:

- ☐ The study may be conducted on larger agricultural fields so that different soil salinity indices derived from the Landsat data could be tested.
- ☐ Impact of soil salinity on shallow rooted crops should also be determined through remotely sensed data
- ☐ The concerned government agencies and policymakers should use the remotely sensed data for the prediction of the crop yields from the agricultural fields of Pakistan with varying degrees of soil salinity.

REFERENCES

- Abbas, A., Khan, S., Hussain, N., Hanjra, M. A., & Akbar, S. (2013). Characterizing soil salinity in irrigated agriculture using a remote sensing approach. *Physics and Chemistry of the Earth, Parts A/B/C*, 55: 43-52.
- Alam, S.M., and Ansari, R. (2000). Agricultural land scenario of Sindh province. *Pakistan economist*. <http://pakistaneconomist.com/issue2000//issue25/i&e2.htm> (visited on Nov. 5, 2019).
- Aldakheel, Y.Y. (2011). Assessing NDVI spatial pattern as related to irrigation and soil salinity management in Al-Hassa Oasis, Saudi Arabia. *J. Indian Soc. Remote Sensing*, 39(2): 171- 180.
- Allbed, A., and L. Kumar. (2013). Soil salinity mapping and monitoring in arid and semi-arid regions using remote sensing technology: A review. *Adv. Remote Sensing*, 2: 373-385.
- Badgley, G., Field, C. B., & Berry, J. A. (2017). Canopy near-infrared reflectance and terrestrial photosynthesis. *Science Advances*, 3(3): e1602244.
- Bastiaanssen, W.G.M., Menenti, M., Feddes, R.A., and Holtslag, A.A.M. (1998a). A remote sensing surface energy balance algorithm for land (SEBAL): Part 1: Formulation. *J. Hydrol.* 212: 198–212.
- Bastiaanssen, W.G.M., Pelgrum, H., Wang, J., Ma, Y., Moreno, J.F., Roerink, G.J., and van der Wal, T. (1998b). A remote sensing surface energy balance algorithm for land (SEBAL) Part 2: Validation. *J. Hydrol.* 212-Part2: 213-229.
- Bennett, D.L., George, R.J., and Whitfield, B. (2000). The use of ground EM systems to accurately assess salt store and help define land management options for salinity management. *Explor. Geophys.* 31: 249–254.
- Boegh, E., Soegaard, H., Broge, N., Hasager, C., Jensen, N., Schelde, K., and Thomsen, A. (2002). Airborne multi-spectral data for quantifying leaf area index, nitrogen concentration and photosynthetic efficiency in agriculture. *Remote Sensing of Environment*, 81(2-3): 179-193.
- Bouyoucos, G.J. (1936). Directions for making mechanical analysis of soils by the hydrometer method. *Soil Science* 4: 225 – 228.
- Crippen, R. (1990). Calculating the vegetation index faster. *Remote Sensing of Environment*, 34: 71-73.
- Dale, P., Hulsman, K., Chandica, A.L. (1986). Classification of reflectance on color

infrared aerial photographs and sub-tropical salt-marsh vegetation types. *Int. J. Remote Sensing*, 7(12): 1783-1788.

Drisya, J., & Roshni, T. (2018). Spatiotemporal variability of soil moisture and drought estimation using a distributed hydrological model. In: *Integrating Disaster Science and Management* (pp. 451-460). Elsevier.

Eldiery, A., Garcia, L. A., & Reich, R. M. (2005). Estimating soil salinity from remote sensing data in cornfields. *Hydrology Days*, 970: 31-42.

Elhaddad, A., Garcia, L. A., and Chávez, J. L. (2010). Using a surface energy balance model to calculate spatially distributed actual evapotranspiration. *J. Irrig. Drain. Engg.*, 137(1): 17-26.

Gates, T. K., Garcia, L. A., Hemphill, R. A., Morway, E. D., and Elhaddad, A. (2012). Irrigation practices, water consumption, & return flows in Colorado's Lower Arkansas River Valley: Field and model investigations. *Colorado Water Institute Completion Report No. 221*, Colorado Agricultural Experiment Station No. TR-12, Colorado State Univ., Fort Collins, Colorado.

Gitelson, A. (2004). Wide dynamic range vegetation index for remote quantification of biophysical characteristics of vegetation. *Journal of Plant Physiology* 161(2): 165-173.

Gleason, D.J., Andales, A.A., Bauder, T., Chávez, J.L. (2013). Performance of atmometers in estimating reference evapotranspiration in a semi-arid environment. *Agric. Water Management*, 130:27-35.

Gorji, T., Tanik, A. and Sertel, E. 2015. Soil salinity prediction, monitoring, and mapping using modern technologies. *Procedia Earth and Planetary Science*, 15: 507-512.

Gowda, P. H., Chávez, J. L., Colaizzi, P. D., Evett, S. R., Howell, T. A., and Tolk, J. (2008). ET mapping for agricultural water management: Present status and challenges. *Irrig. Sci.*, 26(3): 223–237.

Gupta, B., & Huang, B. (2014). Mechanism of salinity tolerance in plants: physiological, biochemical, and molecular characterization. *International journal of genomics*, 2014.

Hamzeh, S., Naseri, A.A., AlaviPanah, S.K., Bartholomeus, H., and Herold, M. (2016). Assessing the accuracy of hyperspectral and multispectral satellite imagery for categorical and quantitative mapping of salinity stress in sugarcane fields. *Inter. J. Applied Earth Observation and Geoinformation*, 52:412-421.

Hanson, B.R.; Kaita, K. (1997). Response of electromagnetic conductivity meter to soil salinity and soil-water content. *J. Irrig. Drain. Eng.—ASCE*, 123: 141–143.

- Henebry, G. M., Viña, A., & Gitelson, A. A. (2004). The wide dynamic range vegetation index and its potential utility for gap analysis. *Gap Analysis Bulletin* 12: 50-56.
- Huete, A. (1988). A soil-adjusted vegetation index (SAVI). *Remote Sensing of Environment*, 25: 295-309.
- Jordan, C. F. (1969). Derivation of leaf-area index from quality of light on the forest floor. *Ecology*, 50(4): 663-666.
- Khan, G.S. (1998). Soil salinity/sodicity status in Pakistan. *Soil Survey of Pakistan*, Lahore. p 59.
- Knipling, E. B. (1970). Physical and physiological basis for the reflectance of visible and near-infrared radiation from vegetation. *Remote Sensing of Environment*, 1(3): 155-159.
- Kustas, W. P., and Norman, J. M. (2000). A two-source energy balance approach using directional radiometric temperature observations for sparse canopy-covered surfaces. *Agron J.* 92: 847–854.
- Lesch S.M., Rhoades J.D., Corwin D.L., Robinson, D.A., and Suárez D.L. (2002). ESAP-SaltMapper version 2.30R. User manual and tutorial guide. *Res. Report 149, December 2002. USDA-ARS. George E. Brown, Jr., Salinity Laboratory, Riverside, California.*
- Lesch, S.M., Rhoades, J.D., and Corwin, D.L. (2000). The ESAP Version 2.01r user manual and tutorial guide. *Research Report #146. George E. Brown Jr., Salinity Laboratory, Riverside, CA*, 153pp.
- Lesch, S.M., Strauss, D.J., and Rhoades, J.D. (1995). Spatial prediction of soil salinity using electromagnetic induction techniques 2. An efficient spatial sampling algorithm suitable for multiple linear regression model identification and estimation. *Water Resour. Res.*, 31(2): 387-398.
- Major, D.J., Baret, F., and Guyot, G. (1990). A ratio vegetation index adjusted for soil brightness. *International Journal of Remote Sensing*, 11(5): 727–740.
- Metternich, G. I., and Zinck, J. A. 2003. Remote sensing of soil salinity: Potentials and constraints. *Remote Sensing Environ.*, 85: 1–20.
- Mkhwanazi, M., Chávez, J.L., and Andales, A.A. (2015). SEBAL-A: A remote sensing *ET* algorithm that accounts for advection with limited data. Part I: Development and validation. *Remote Sens.*, 7(11): 15046-15067; doi:10.3390/rs71115046.
- Oliveira, A. B., Alencar, N. L. M., & Gomes-Filho, E. (2013). Comparison between

the water and salt stress effects on plant growth and development. Responses of organisms to water stress, 67.

Postel, S. (1999). *Pillar of Sand: Can the Irrigation Miracle Last?* W.W. Norton and Co., New York, NY.

Qi, J., Chehbouni, A., Huete, A., Kerr, Y., and Sorooshian, S. (1994). A modified soil adjusted vegetation index. *Remote Sensing of Environment*, 48: 119-126.

Qureshi, A.S. (2011). Water management in the Indus Basin in Pakistan: Challenges and opportunities. *Mountain Res. Dev.* 31(3): 252-260.

Rhoades, J.D. (1996). Salinity: Electrical conductivity and total dissolved solids. In *Methods of Soil Analysis, Part 3 – Chemical Methods*. Soil Science Society of America, Madison, Wisconsin, pp. 417-435.

Rondeaux, G., Steven, M., & Baret, F. (1996). Optimization of soil-adjusted vegetation indices. *Remote sensing of environment*, 55(2), 95-107.

Rouse, J., Haas, R., Schell, J., and Deering, D. (1973). Monitoring vegetation systems in the Great Plains with ERTS. *Third ERTS Symposium*, NASA: 309-317.

Scudiero, E., Corwin, D.L., Skaggs, T.H. (2015). Regional-scale soil salinity assessment using Landsat ETM+ canopy reflectance. *Remote Sens. Environ.*, 169: 335–43.

Scudiero, E., Skaggs, T.H., Corwin, D.L. (2014). Regional scale soil salinity evaluation using Landsat 7, western San Joaquin Valley, California, USA. *Geoderma Regional* 2–3: 82–90.

Siyal, A. A., Siyal, A. G., & Abro, Z. A. (2002). Salt affected soils, their identification and reclamation. *Pak. J. Appl. Sci.*, 2(5): 537-540.

Sripada, R. P., Heiniger, R. W., White, J. G., & Meijer, A. D. (2006). Aerial color infrared photography for determining early in-season nitrogen requirements in corn. *Agronomy Journal*, 98(4): 968-977.

Srivastava, A., Tripathi, N.K., and Gokhale, K.V.G.K. (1997). Mapping groundwater salinity using IRS-1B LISS II data and GIS techniques. *Int. J. Remote Sensing*, 18 (13): 2853-2862.

Szabolcs, I. (1989). *Salt-Affected Soils*. CRC Press, Boca Raton, FL.

Teggi, S., Costanzini, S., Despini, F., Chiodi, P. and Immordino, F. (2012). SPOT5 imagery for soil salinity assessment in Iraq. In: *SPIE Remote Sensing* (pp. 85380V-85380V). *Inter. J. Soc. Optics and Photonics*.

Tucker, C. (1979). Red and photographic infrared linear combinations for monitoring vegetation. *Remote Sensing of Environment* 8: 127–150.

Turnham, C. (2003). Using electromagnetic induction methods to measure just a bullet point agricultural soil salinity and its effects on adjacent native vegetation in Western Australia. B.Sc. Thesis, Lancaster University, Lancashire, UK.

Wallender, W. W., and Tanji, K. K. (2012). Agricultural salinity assessment and management. 2nd Ed., *ASCE Manuals, and Reports on Engrg. Practice No. 71*, Am. Soc. Civil Engineers, Reston, Virginia.

Wittler, J. M., Cardon, G. E., Gates, T. K., Cooper, C. A., and Sutherland, P. L. (2006). Calibration of electromagnetic induction for regional assessment of soil water salinity in an irrigated valley. *J. Irrig. Drain. Engg.*, 132(5): 436 – 444.

Yao, R., & Yang, J. (2010). Quantitative evaluation of soil salinity and its spatial *distribution using an electromagnetic induction method*. *Agricultural Water Management*. 97(12): 1961-1970.

Zhu, J.K. (2001). Plant salt tolerance. *Trends in Plant Science*, 6(2): 66-71.

Annexure-1

1.1 Climatic data for October 2018

DRAINAGE AND RECLAMATION INSTITUTE OF PAKISTAN (DRIP) CAMPUS, TANDO JAM														
METEOROLOGICAL DATA														
October, 2018														
Date	Average Daily Temp Co		RH %		Pan Evap. 24 hrs (mm)	ETP Daily (mm)	Wind Velocity Average Knot/hr	Wind Direction			Sunshine Hours		Rain Fall (mm)	Remarks
	Min.	Max.	Min.	Max.				9 A.M	12 noon	5 P.M	Hr.	Mint		
1	23.0	38.0	54	84	5.84	5.450	2.4	SSW	SSW	SSW	10	15		
2	24.0	38.0	64	92	6.09	5.128	2.2	SSW	SSW	SSW	10	5		
3	24.0	36.0	63	92	5.58	5.239	3.1	SSW	SSW	SSW	10	5		
4	24.0	36.0	54	92	5.84	5.398	2.8	SSW	SSW	SSW	10	30		
5	23.0	39.0	46	92	6.09	5.220	1.5	SSW	SSW	SSW	10	30		
6	20.0	38.0	53	92	5.84	4.724	1.0	SSW	SSW	SSW	10	25		
7	19.0	41.0	53	84	6.09	4.637	0.3	SSW	SSW	SSW	10	10		
8	19.0	41.0	31	84	5.84	5.026	1.4	NNE	SSW	SSW	9	0		
9	25.0	35.0	47	85	5.08	4.527	2.0	SSW	SSW	SSW	6	30		Couldday day
10	24.0	34.0	51	84	4.82	4.329	1.3	SSW	SSW	SSW	7	30		Couldday day
11	20.0	35.0	52	91	3.30	4.233	0.5	SSW	SSW	SSW	9	30		
12	20.0	35.0	52	75	4.31	4.674	1.0	NNW	NNW	NNW	10	10		
13	21.0	35.0	61	91	5.85	4.771	1.5	NNW	NNW	NNW	9	35		
14	20.0	39.0	52	91	4.57	4.797	0.8	NNW	NNW	NNW	10	10		
15	20.0	37.0	49	92	4.57	3.789	0.8	SSW	SSW	SSW	6	0		Couldday day
16	23.0	36.0	48	92	4.57	4.331	0.5	SSW	SSW	SSW	8	55		Couldday day
17	21.0	36.0	43	92	4.82	4.266	0.7	SSW	SSW	SSW	8	40		Couldday day
18	23.0	36.0	43	92	4.82	4.833	0.7	NEE	NNE	NNE	10	10		
19	20.0	35.0	37	91	4.82	4.480	0.4	NNW	NNW	NNW	10	40		
20	19.0	35.0	4	75	4.57	4.602	0.6	NEE	NEE	NEE	10	10		
21	16.0	36.0	49	68	4.82	4.084	0.3	SWW	SWW	SWW	9	0		
22	15.0	35.0	42	83	4.57	4.315	7.0	SWW	SWW	SWW	10	30		
23	20.0	39.0	29	91	4.38	4.588	0.5	SWW	SWW	SWW	9	35		
24	22.0	36.0	48	92	4.57	4.731	1.4	SSW	SSW	SSW	9	45		
25	20.0	36.0	38	91	4.57	4.794	1.3	SSW	SSW	SSW	10	0		
26	20.0	36.0	38	91	3.93	4.656	0.6	SSW	SSW	SSW	10	15		
27	19.0	38.0	42	91	4.44	4.622	0.6	NNE	NNE	NWW	10	30		
28	19.0	38.0	42	91	3.81	4.590	0.7	SWW	SWW	SWW	10	0		
29	19.0	38.0	32	91	4.69	4.525	0.5	NNW	NNW	NNW	9	35		
30	19.0	36.0	42	91	4.19	4.389	0.5	SWW	SWW	SWW	9	45		
31	19.0	36.0	42	91	4.06	4.389	0.5	SSW	SSW	SSW	9	40		
Total	640.0	1139.0	1401.0	2734.0	151.3	144.1	39.4				286.0	695.0		
Mean	21	37	45	88	4.9	4.6	1.3				9.2	22		
RH = Relative Humidity														
ETp = Potential Evapotranspiration (Modified Penman Method)														

1.2 Climatic data for November 2018

DRAINAGE AND RECLAMATION INSTITUTE OF PAKISTAN (DRIP) CAMPUS, TANDO JAM														
METEOROLOGICAL DATA														
November, 2018														
Date	Average Daily Temp Co		RH %		Pan Evap. 24 hrs (mm)	ETP Daily (mm)	Wind Velocity Average	Wind Direction			Sunshine Hours		Rain Fall (mm)	Remarks
	Min.	Max.	Min.	Max.			Knot/hr	9 A.M	12 noon	5 P.M	Hr.	Mint		
1	19	36	52	91	3.81	3.571	0.4	NNW	NNW	NNW	9	35		
2	19	36	42	91	3.81	3.573	0.2	NNW	NNW	NNW	9	40		
3	19	32	47	65	4.57	3.825	1	NNW	NNW	NNW	9	45		
4	18	32	57	63	4.31	3.908	1.4	NNW	NNW	NNW	10	5		
5	15	31	37	70	4.31	3.856	1.4	NNW	NNW	NNW	10	25		
6	15	31	32	70	3.81	3.533	0.8	NNW	NNW	NNW	9	35		
7	11	33	35	90	3.81	3.25	0.5	SSE	SSE	SSE	10	0		
8	11	32	49	90	3.55	3.17	1	SSE	SSE	SSE	9	15		
9	15	32	49	90	3.04	3.106	0.4	NNW	NNW	NNW	8	50		Coulday Day
10	15	34	42	90	2.79	3.165	0.4	NNW	NNW	NNW	8	10		Coulday Day
11	16	35	37	100	2.79	3.391	0.4	SSE	SSE	SSE	9	25		
12	19	35	50	91	3.04	2.273	0.3	NNW	NNW	NNW	1	45		Coulday Day
13	19	32	49	100	2.28	1.999	0.4	SSE	SSE	SSE	0	0		Coulday Day
14	19	31	53	90	2.28	1.577	0.7	NNW	NNW	NNW	2	5		Coulday Day
15	19	30	47	73	2.28	3.666	1.1	NNW	NNW	NNW	9	55		
16	15	32	37	80	3.81	3.514	0.9	NNW	NNW	NNW	9	10		
17	15	32	64	91	2.54	2.932	0.2	NNW	NNW	NNW	9	5		
18	16	32	45	100	2.54	3.188	0.4	SSE	SSE	SSE	8	25		Coulday Day
19	17	30	53	80	2.54	3.159	0.6	NNW	NNW	NNW	9	10		
20	17	28	64	80	4.82	3.447	2	NNW	NNW	NNW	9	0		
21	19	31	56	72	7.62	3.872	2.2	NNW	NNW	NNW	8	0		Coulday Day
22	15	32	39	90	3.3	3.42	0.5	SSE	SSE	SSE	10	30		
23	19	32	34	72	4.31	3.764	0.8	NNW	NNW	NNW	9	35		
24	17	32	45	80	3.55	3.795	1.6	NNW	NNW	NNW	9	45		
25	15	31	50	90	2.79	2.598	0.3	SSE	SSE	SSE	5	10		Coulday Day
26	16	31	48	100	1.77	2.606	0.4	SSE	SSE	SSE	5	15		Coulday Day
27	19	28	64	91	2.28	2.374	0.3	SSE	SSE	SSE	4	10		Coulday Day
28	16	28	51	100	1.77	3.211	0.3	NNW	NNW	NNW	9	15		
29	16	26	62	80	3.17	3.102	1.5	NNW	NNW	NNW	8	0		Coulday Day
30	16	30	52	90	3.55	3.517	1.9	NNW	NNW	NNW	9	10		
Total	497	947	1442	2560	100.84	96.362	24.3				232	610		
Mean	16	31	47	83	3.25	3.11	0.8				7.5	20		
RH = Relative Humidity														
ETp = Potential Evapotranspiration (Modified Penman Method)														

1.3 Climatic data for December 2018

DRAINAGE AND RECLAMATION INSTITUTE OF PAKISTAN (DRIP) CAMPUS, TANDO JAM														
METEOROLOGICAL DATA														
December, 2018														
Date	Average Daily Temp Co		RH %		Pan Evap. 24 hrs (mm)	ETP Daily (mm)	Wind Velocity Average Knot/hr	Wind Direction			Sunshine Hours		Rain Fall (mm)	Remarks
	Min.	Max.	Min.	Max.				9 A.M	12 noon	5 P.M	Hr.	Mint		
1	12	31	50	100	3.81	2.634	0.5	SWW	SWW	SWW	9	20		
2	13	31	50	100	2.03	2.573	0.6	SSE	SSE	SSE	8	5		Coulday Day
3	13	29	51	90	2.28	2.746	1.1	NNW	NNW	NNW	8	40		Coulday Day
4	15	26	55	90	2.79	2.838	1.5	NNW	NNW	NNW	9	30		
5	15	27	63	80	2.79	2.773	0.9	NNW	NNW	NNW	9	50		
6	15	29	58	100	3.04	2.58	0.3	SSE	SSE	SSE	9	15		
7	15	27	63	90	3.04	2.683	1.1	NNW	NNW	NNW	9	30		
8	13	28	68	89	3.04	2.433	0.7	SSE	SSE	SSE	8	10		Coulday Day
9	15	28	68	92	2.54	2.321	0.2	SSW	SSW	SSW	7	25		Coulday Day
10	17	27	56	90	2.79	2.52	0.2	SSW	SSW	SSW	8	10		Coulday Day
11	15	24	60	89	2.54	2.433	1.4	NNW	NNW	NNW	6	40		Coulday Day
12	14	23	59	89	2.79	2.607	1.9	NNW	NNW	NNW	8	0		Coulday Day
13	11	24	53	89	2.79	2.517	1	NNW	NNW	NNW	9	40		
14	11	24	39	78	2.54	2.674	0.7	NNW	NNW	NNW	10	10		
15	9	23	43	77	2.79	2.745	1.5	NNW	NNW	NNW	9	50		
16	11	23	51	78	2.79	3.047	2.6	NNW	NNW	NNW	9	40		
17	11	23	45	88	2.79	2.958	2.3	NNW	NNW	NNW	10	5		
18	9	24	39	77	3.04	2.865	1.7	NNW	NNW	NNW	9	30		
19	4	27	26	87	2.54	2.539	0.7	SSW	SSW	SSW	10	0		
20	8	25	47	77	2.79	2.631	1.2	NNW	NNW	NNW	9	30		
21	11	24	39	77	2.79	2.874	1.4	NNW	NNW	NNW	9	30		
22	11	24	82	76	2.54	2.401	1.1	NNW	NNW	NNW	9	30		
23	11	24	72	76	2.28	2.375	0.9	NNW	NNW	NNW	8	55		Coulday Day
24	11	22	51	76	2.79	2.821	2.2	NNW	NNW	NNW	8	30		Coulday Day
25	11	24	57	76	2.28	2.687	1.6	NNW	NNW	NNW	8	35		Coulday Day
26	11	27	38	88	2.03	2.639	0.6	NNW	NNW	NNW	9	40		
27	7	26	30	88	2.41	2.505	1	SWW	SWW	SWW	7	55		Coulday Day
28	6	26	47	77	2.03	2.302	0.3	SSW	SSW	SSW	8	40		Coulday Day
29	6	27	59	87	2.03	2.225	0.4	NNW	NNW	NNW	9	30		
30	7	25	51	88	2.03	2.3	0.6	SSW	SSW	SSW	9	0		
31	6	24	53	87	1.77	2.237	0.9	NNW	NNW	NNW	8	30		Coulday Day
Total	344	796	1623	2646	80.53	80.483	33.1				265	855	0	
Mean	11	26	52	85	2.60	2.60	1.1				8.5	28	0	
RH = Relative Humidity														
ETp = Potential Evapotranspiration (Modified Penman Method)														

1.4 Climatic data for January 2019

DRAINAGE AND RECLAMATION INSTITUTE OF PAKISTAN (DRIP) CAMPUS, TANDO JAM														
METEOROLOGICAL DATA														
January, 2019														
Date	Average Daily Temp Co		RH %		Pan Evap. 24 hrs (mm)	ETP Daily (mm)	Wind Velocity Average	Wind Direction			Sunshine Hours		Rain Fall (mm)	Remarks
	Min.	Max.	Min.	Max.			Knot/hr	9 A.M	12 noon	5 P.M	Hr.	Mint		
1	10	26	42	88	1.77	2.928	1.4	NNW	NNE	NNE	9	25		
2	12	26	49	88	2.03	2.775	0.9	NNW	NNE	NNE	9	0		
3	12	26	49	88	2.79	2.786	0.9	NNW	NNE	NNE	9	5		
4	13	26	55	89	2.41	2.75	0.8	NNW	NNE	NNE	3	40		Coulday day
5	15	25	58	69	2.03	2.494	1.9	SSW	SSW	SSW	0	45		Coulday day
6	10	22	62	87	2.79	2.578	1.8	NNW	NNE	NNE	8	50		Coulday day
7	11	21	49	88	2.28	2.59	1.3	SSW	SSW	SSW	8	30		Coulday day
8	11	22	51	88	2.03	2.509	0.9	NNW	NNE	NNE	8	30		Coulday day
9	10	24	46	76	2.54	2.448	0.4	NNW	NNE	NNE	7	30		Coulday day
10	11	27	56	88	2.41	2.165	0.1	SSW	SSW	SSW	5	30		Coulday day
11	16	22	66	70	2.54	2.585	2.7	NNW	NNE	NNE	0	0		Coulday day
12	15	22	66	80	2.41	2.632	1.6	NNW	NNE	NNE	7	5		Coulday day
13	11	23	56	77	2.54	2.474	0.4	NNW	NNE	NNE	8	40		Coulday day
14	11	23	45	88	2.54	3.301	3.2	NNW	NNE	NNE	9	20		
15	11	26	36	88	2.79	2.951	1.2	NNW	NNE	NNE	9	30		
16	11	25	54	88	2.54	2.542	0.4	SSW	SSW	SSW	9	10		
17	12	23	59	77	3.3	2.729	1	NNW	NNE	NNE	9	30		
18	11	25	54	88	3.04	2.839	1.9	NNW	NNE	NNE	8	30		Coulday day
19	11	24	56	88	1.52	2.567	1	NNW	NNE	NNE	8	35		Coulday day
20	11	26	51	88	2.28	2.71	1.3	NNW	NNE	NNE	7	45		Coulday day
21	13	17	70	100	Nil	1.518	1.8	NNW	NNE	NNE	1	15	27.08	Coulday day
22	9	22	36	100	0.5	2.341	0.5	NEE	NNE	NNE	8	0		Coulday day
23	7	22	51	100	3.81	2.327	0.8	SSW	SSW	SSW	9	30		
24	9	22	43	87	5.08	2.681	1	NNE	NNE	NNE	10	10		
25	10	22	51	87	2.79	2.617	1.1	NW	NNE	NNE	9	45		
26	7	22	64	87	2.54	2.164	0.3	NNW	NNE	NNE	8	40		Coulday day
27	11	22	64	76	2.54	2.711	1.2	NNE	NNE	NNE	10	0		
28	11	24	46	88	2.28	2.711	0.8	NNW	NNE	NNE	9	50		
29	7	25	41	87	2.28	2.501	0.4	NNW	NNE	NNE	9	30		
30	11	26	36	88	2.28	2.483	0.6	SSW	SSW	SSW	6	0	0.8	Coulday day
31	12	21	57	88	2.03	2.818	2.7	NNW	NNE	NNE	8	0		Coulday day
Total	342	729	1619	2669	74.71	80.225	36.3				227	750	27.88	
Mean	11	24	52	86	2.4	2.6	1.2				7.3	24	0.9	
RH = Relative Humidity														
ETp = Potential Evapotranspiration (Modified Penman Method)														

1.5 Climatic data for February 2019

DRAINAGE AND RECLAMATION INSTITUTE OF PAKISTAN (DRIP) CAMPUS, TANDO JAM														
METEOROLOGICAL DATA														
February, 2019														
Date	Average Daily Temp Co		RH %		Pan Evap. 24 hrs (mm)	ETP Daily (mm)	Wind Velocity Average	Wind Direction			Sunshine Hours		Rain Fall (mm)	Remarks
	Min.	Max.	Min.	Max.				9 A.M	12 noon	5 P.M	Hr.	Mint		
1	10	21	65	87	2.79	3.058	1.8	NNW	NNW	NNW	9	30		
2	10	22	64	87	3.04	3.549	1.9	NNW	NNW	NNW	10	5		
3	11	22	73	77	3.04	3.3	2	NNW	NNW	NNW	10	0		
4	11	24	39	76	2.79	3.751	1.7	NNW	NNW	NNW	10	15		
5	11	25	51	88	3.55	3.31	0.9	SSW	SSW	SSW	10	10		
6	14	26	30	58	2.54	3.687	0.7	SSW	SSW	SSW	9	10		
7	7	26	30	73	4.31	3.545	1.3	NNW	NNW	NNW	9	40		
8	8	23	19	74	3.3	3.397	0.8	NNW	NNW	NNW	10	15		
9	9	25	36	74	4.06	3.812	1.9	NNW	NNW	NNW	10	5		
10	7	26	38	74	2.79	3.226	0.4	NNW	NNW	NNW	10	10		
11	9	25	35	63	2.79	3.229	0.2	NNW	NNW	NNW	10	0		
12	9	25	47	75	3.81	3.69	1.9	NNW	NNW	NNW	10	20		
13	14	25	41	78	4.57	4.356	3.1	NNW	NNW	NNW	9	50		
14	13	26	49	77	3.55	3.783	1.8	SSW	SSW	SSW	9	40		
15	12	26	42	78	2.79	3.414	0.5	SSW	SSW	SSW	10	10		
16	10	26	38	87	3.55	3.448	1	NNW	NNW	NNW	10	10		
17	11	28	46	88	3.3	2.965	0.4	SSW	SSW	SSW	7	5		Couldady day
18	11	29	46	88	4.06	3.788	2.9	SSW	SSW	SSW	7	40		Couldady day
19	15	29	52	89	4.31	3.678	2.5	SSW	SSW	SSW	7	0		Couldady day
20	17	26	57	80	3.55	3.311	2	NNW	NNW	NNW	5	10		Couldady day
21	17	24	64	90	3.55	3.353	2.5	NNW	NNW	NNW	7	30		Couldady day
22	11	26	61	88	3.55	3.254	1.4	NNW	NNW	NNW	9	5		
23	13	26	59	78	4.57	3.499	1.8	NNW	NNW	NNW	8	30		Couldady day
24	15	26	53	79	3.3	3.587	0.8	NNW	NNW	NNW	10	25		
25	11	28	51	88	3.04	3.127	0.5	NNW	NNW	NNW	8	40		Couldady day
26	15	27	50	89	3.3	3.638	0.9	NNW	NNW	NNW	10	35		
27	15	27	63	79	4.31	3.859	1.8	NNW	NNW	NNW	10	45		
28	11	27	38	88	3.81	2.302	0.6	SSW	SSW	SSW	8	15		Couldady day
Total	327	716	1337	2250	97.92	96.916	40				251	550		
Mean	11	23	43	73	3.2	3.1	1.3				8.1	18		
RH = Relative Humidity														
ETp = Potential Evapotranspiration (Modified Penman Method)														

1.6 Climatic data for March 2019

DRAINAGE AND RECLAMATION INSTITUTE OF PAKISTAN (DRIP) CAMPUS, TANDO JAM														
METEOROLOGICAL DATA														
March, 2019														
Date	Average Daily Temp Co		RH %		Pan Evap. 24 hrs (mm)	ETP Daily (mm)	Wind Velocity Average Knot/hr	Wind Direction			Sunshine Hours		Rain Fall (mm)	Remarks
	Min.	Max.	Min.	Max.				9 A.M	12 noon	5 P.M	Hr.	Mint		
01	12.0	29.0	40	78	4.57	3.725	0.9	SSE	SSE	SSE	6	50		Coulday day
02	15.0	22.0	71	89	5.08	3.137	1.8	NW	NWW	NWW	5	20	5	Coulday day
03	13.5	21.0	71	89	Nil	3.325	3.3	NNW	NNW	NNW	5	30		Coulday day
04	13.0	25.0	61	89	5.33	4.260	2.5	NNW	NNW	NNW	9	55		
05	12.0	29.0	40	78	3.04	4.330	0.8	SSW	SSW	SSW	10	0		
06	15.0	30.0	36	90	3.81	4.544	0.8	SWW	SWW	SWW	10	35		
07	15.0	29.0	35	90	4.82	4.421	0.7	SSW	SSW	SSW	10	15		
08	15.0	28.0	45	90	5.58	4.582	1.7	NNW	NNW	NNW	10	0		
09	15.0	28.0	68	90	5.02	4.329	1.9	NNW	NNW	NNW	10	0		
10	15.0	29.0	61	90	4.31	3.642	0.7	NWW	NWW	NWW	7	10		Coulday day
11	15.0	29.0	39	90	4.06	4.654	1.3	NNW	NNW	NNW	10	35		
12	15.0	29.0	29	80	4.82	4.038	1.0	NNW	NNW	NNW	6	35		Coulday day
13	15.0	26.0	49	70	4.82	4.507	1.6	NEE	NEE	NEE	9	40		
14	12.0	28.0	45	89	5.08	4.535	1.9	NEE	NEE	NEE	10	40		
15	15.0	29.0	40	89	5.08	4.790	1.7	NEE	NEE	NEE	10	25		
16	16.0	29.0	47	71	5.84	4.782	1.9	NNE	NNE	NNE	9	0		
17	16.0	31.0	50	80	4.57	4.719	1.2	NEE	NEE	NEE	10	12		
18	15.0	34.0	32	71	4.82	4.754	0.4	NWW	NWW	NWW	10	20		
19	15.0	34.0	27	80	5.08	4.818	0.6	SSW	SSW	SSW	10	50		
20	19.0	32.0	39	82	6.60	6.437	4.5	SWW	SWW	SWW	10	25		
21	19.0	32.0	39	82	5.84	5.240	1.7	NNW	NNW	NNW	10	15		
22	19.0	34.0	32	82	5.33	5.374	2.0	NEE	NEE	NEE	9	25		
23	19.0	37.0	35	74	5.58	5.281	0.9	SSW	SSW	SSW	10	15		
24	20.0	34.0	42	82	5.33	4.458	1.9	NWW	NWW	NWW	5	20		Coulday day
25	20.0	34.0	36	82	5.58	5.318	1.8	NEE	NEE	NEE	9	35		
26	20.0	35.0	37	66	5.33	5.385	1.4	SSE	SSE	SSE	9	35		
27	20.0	40.0	23	82	5.58	5.496	0.7	SSW	SSW	SSW	10	30		
28	20.0	41.0	30	75	7.11	5.875	1.4	SSW	SSW	SSW	10	20		
29	23.0	42.0	31	76	6.35	5.412	1.3	SSW	SSW	SSW	7	30		Coulday day
30	19.0	40.0	38	61	8.12	6.186	1.7	SSW	SSW	SSW	11	15		
31	19.0	38.0	37	82	6.35	5.399	1.1	NWW	NWW	NWW	10	40		
Total	511.5	978.0	1305.0	2519.0	158.8	147.8	47.1				276.0	777.0	5.0	
Mean	17	32	42	81	5.1	4.8	1.5				8.9	25	0.2	
RH = Relative Humidity														
ETp = Potential Evapotranspiration (Modified Penman Method)														

1.7 Climatic data for April 2019

DRAINAGE AND RECLAMATION INSTITUTE OF PAKISTAN (DRIP) CAMPUS, TANDO JAM														
METEOROLOGICAL DATA														
April, 2019														
Date	Average Daily Temp Co		RH %		Pan Evap. 24 hrs (mm)	ETP Daily (mm)	Wind Velocity Average Knot/hr	Wind Direction			Sunshine Hours		Rain Fall (mm)	Remarks
	Min.	Max.	Min.	Max.				9 A.M	12 noon	5 P.M	Hr.	Mint		
1	19	41	21	61	6.6	6.09	0.7	SSW	SSW	SSW	10	35		
2	20	41	31	68	5.58	6.022	0.6	NNE	NNE	NNE	10	55		
3	23	41	24	84	7.62	6.699	1.7	SSW	SSW	SSW	10	15		
4	22	43	20	76	6.35	6.638	0.9	SSW	SSW	SSW	11	15		
5	23	41	31	91	8.63	6.397	1.8	SSW	SSW	SSW	9	30		
6	25	41	44	92	7.62	7.069	3.7	SSW	SSW	SSW	9	0		
7	24	42	40	92	6.6	6.357	1.9	SSW	SSW	SSW	9	10		
8	25	41	31	84	7.36	7.374	2.9	SSW	SSW	SSW	10	20		
9	23	40	34	91	6.6	6.263	2.2	SSW	SSW	SSW	8	55		
10	24	42	22	76	7.36	8.604	4.5	SSW	SSW	SSW	10	20		
11	24	42	25	84	8.63	7.69	3.3	SSW	SSW	SSW	10	20		
12	23	42	28	77	9.39	7.517	3.1	NNW	NNW	NNW	10	10		
13	24	38	42	76	7.62	6.148	1.7	SSW	SSW	SSW	9	0		
14	23	37	46	70	6.35	5.444	1.3	SSW	SSW	SSW	7	15		Coulday day
15	27	31	27	51	8.12	5.729	2.7	SSW	SSW	SSW	2	40		Coulday day
16	23	33	45	84	7.87	6.945	5	SSW	SSW	SSW	9	40		
17	20	32	44	91	4.31	6.193	2.9	SSW	SSW	SSW	11	15	2.3	
18	20	34	45	76	6.09	6.087	1.6	NNE	NNE	NNE	11	30		
19	23	36	34	76	6.09	6.278	1.1	SSW	SSW	SSW	11	10		
20	23	38	37	92	8.63	6.745	2.3	SSW	SSW	SSW	11	20		
21	23	38	37	92	8.12	7.096	3.2	SSW	SSW	SSW	11	20		
22	24	41	35	76	7.87	8.346	4.4	SSW	SSW	SSW	11	30		
23	24	41	35	76	8.87	8.064	3.7	SSW	SSW	SSW	11	45		
24	25	38	54	92	6.85	7.425	4.7	SSW	SSW	SSW	11	20		
25	27	40	50	92	7.36	8.124	5.5	SSW	SSW	SSW	11	10		
26	24	42	22	84	8.12	7.676	2.8	SSW	SSW	SSW	11	0		
27	20	42	32	63	9.9	6.886	1.6	SSW	SSW	SSW	11	30		
28	20	42	32	62	11.93	7.106	2.6	SSW	SSW	SSW	11	10		
29	23	42	35	63	7.63	6.96	1.4	SSW	SSW	SSW	11	25		
30	26	40	34	64	10.16	6.929	3.4	SSW	SSW	SSW	6	0		
Total	694	1182	1037	2356	230.23	206.9	79.2				292	645	2.3	
Mean	23	39	35	79	7.67	6.90	2.6				9.7	22	0.1	
RH = Relative Humidity														
ETp = Potential Evapotranspiration (Modified Penman Method)														

1.8 Climatic data for May 2019

DRAINAGE AND RECLAMATION INSTITUTE OF PAKISTAN (DRIP) CAMPUS, TANDO JAM														
METEOROLOGICAL DATA														
May, 2019														
Date	Average Daily Temp Co		RH %		Pan Evap. 24 hrs (mm)	ETP Daily (mm)	Wind Velocity Average	Wind Direction			Sunshine Hours		Rain Fall (mm)	Remarks
	Min.	Max.	Min.	Max.			Knot/hr	9 A.M	12 noon	5 P.M	Hr.	Mint		
1	20	41	36	76	7.87	6.476	1	NNW	NNW	NNW	10	55		
2	23	40	34	77	7.11	6.573	0.6	SSE	SSE	SSE	11	15		
3	23	40	38	77	7.87	6.619	0.8	SSE	SSE	SSE	11	0		
4	24	41	33	84	6.09	6.757	0.8	NNE	NNE	NNE	11	0		
5	23	42	47	84	9.14	6.76	1	SSW	SSW	SSW	11	0		
6	27	39	50	85	7.87	8.034	4.3	SSW	SSW	SSW	11	0		
7	27	39	50	78	9.39	8.434	5.3	SSW	SSW	SSW	10	30		
8	27	37	54	85	9.9	9.731	7.4	SSW	SSW	SSW	11	5		
9	27	38	45	85	10.66	9.19	7.2	SSW	SSW	SSW	11	0		
10	27	37	59	92	8.38	7.778	6.5	SSW	SSW	SSW	10	10		
11	27	36	63	92	10.16	7.581	6.3	SSW	SSW	SSW	10	30		
12	26	39	49	92	9.9	7.839	5.1	SSW	SSW	SSW	10	30		
13	26	40	47	92	8.12	7.802	4.5	SSW	SSW	SSW	10	30		
14	27	40	47	92	9.14	8.829	6.4	SSW	SSW	SSW	11	10		
15	27	38	54	92	11.63	7.941	5.8	SSW	SSW	SSW	10	40		
16	27	37	54	92	9.14	7.156	4	SSW	SSW	SSW	10	25		
17	23	37	49	69	8.63	7.149	2.7	NWW	NWW	NWW	10	20		
18	24	41	45	71	9.39	8.093	3.5	NWW	NWW	NWW	11	0		
19	28	40	45	85	9.9	7.706	4.1	SSW	SSW	SSW	9	30		
20	27	40	47	85	7.87	8.197	4.8	SSW	SSW	SSW	10	15		
21	27	41	52	85	7.62	6.326	0.9	SSW	SSW	SSW	9	15		
22	28	40	47	72	11.17	8.432	4.3	SSW	SSW	SSW	10	40		
23	29	40	47	93	9.9	8.012	4.7	SSW	SSW	SSW	10	15		
24	27	40	47	92	9.39	7.535	3.7	SSW	SSW	SSW	10	30		
25	27	41	45	85	7.62	7.583	3.2	SSW	SSW	SSW	10	0		
26	27	42	47	85	6.6	8.014	3.5	SSW	SSW	SSW	11	5		
27	27	42	40	85	8.63	7.903	4.2	SSW	SSW	SSW	9	10		
28	28	43	49	93	8.63	7.859	3.7	SSW	SSW	SSW	10	30		
29	28	44	50	85	8.89	8.471	4.1	SSW	SSW	SSW	11	0		
30	28	44	50	93	9.14	8.088	4.1	SSW	SSW	SSW	10	40		
31	28	41	56	93	10.16	7.036	3.6	SSW	SSW	SSW	9	0		
Total	814	1240	1476	2646	264.28	239.9	122.1				317	530		
Mean	26	40	48	85	8.53	7.74	3.9				10	17		
RH = Relative Humidity														
ETp = Potential Evapotranspiration (Modified Penman Method)														

1.9 Climatic data for June 2019

DRAINAGE AND RECLAMATION INSTITUTE OF PAKISTAN (DRIP) CAMPUS, TANDO JAM														
METEOROLOGICAL DATA														
June, 2019														
Date	Average Daily Temp Co		RH %		Pan Evap. 24 hrs (mm)	ETP Daily (mm)	Wind Velocity Average	Wind Direction			Sunshine Hours		Rain Fall (mm)	Remarks
	Min.	Max.	Min.	Max.			Knot/hr	9 A.M	12 noon	5 P.M	Hr.	Mint		
1	29	45	56	93	8.89	8.949	3.6	SSW	SSW	SSW	9	40		
2	29	45	57	93	11.43	8.301	4.9	SSW	SSW	SSW	10	40		
3	28	42	57	93	11.93	8.114	5.5	SSW	SSW	SSW	10	35		
4	29	42	70	93	11.17	7.698	6.5	SSW	SSW	SSW	9	55		
5	29	42	65	93	9.39	8.587	6.7	SSW	SSW	SSW	11	25		
6	31	44	61	93	8.63	7.934	3.7	SSW	SSW	SSW	10	40		
7	28	44	61	93	8.38	7.348	2.6	SSW	SSW	SSW	10	35		
8	28	45	48	85	8.38	7.982	2.4	SSW	SSW	SSW	11	20		
9	28	45	53	93	8.63	8.158	3.7	SSW	SSW	SSW	11	5		
10	30	41	47	93	7.87	6.924	5.5	SSW	SSW	SSW	11	30		
11	29	40	61	93	8.89	6.935	5.8	SSW	SSW	SSW	7	20		Coulday Day
12	30	41	47	93	7.87	6.924	5.5	SSW	SSW	SSW	5	10		Coulday Day
13	31	41	56	93	10.66	7.052	1.8	SSW	SSW	SSW	10	0		
14	29	37	56	86	8.89	5.24	2.1	SSW	SSW	SSW	5	15		Coulday Day
15	28	40	51	80	7.11	7.36	1.6	SSW	SSW	SSW	11	45		
16	28	38	69	93	9.65	7.127	3.2	SSW	SSW	SSW	11	15		
17	28	38	75	93	8.12	6.891	3.8	SSW	SSW	SSW	10	55		
18	28	38	65	93	8.38	6.53	3	SSW	SSW	SSW	9	15		
19	30	38	65	86	8.12	6.749	3.4	SSW	SSW	SSW	8	55		Coulday Day
20	29	40	61	93	7.62	6.682	3.5	SSW	SSW	SSW	8	30		Coulday Day
21	28	40	56	93	7.62	7.95	4.7	SSW	SSW	SSW	11	5		
22	28	38	69	93	8.89	7.107	3.3	SSW	SSW	SSW	11	0		
23	29	41	70	93	8.89	7.331	4	SSW	SSW	SSW	10	30		
24	30	39	55	86	8.63	7.673	3.6	SSW	SSW	SSW	10	30		
25	31	39	60	86	8.12	7.698	3.9	SSW	SSW	SSW	10	20		
26	31	41	43	86	8.63	8.05	3.3	SSW	SSW	SSW	10	25		
27	30	40	51	93	9.14	8.093	6	SSW	SSW	SSW	9	10		
28	31	41	47	86	10.66	9.178	6.3	SSW	SSW	SSW	10	20		
29	30	40	64	93	9.9	8.027	6.1	SSW	SSW	SSW	10	35		
30	31	38	74	86	8.12	7.794	6.4	SSW	SSW	SSW	10	5		
Total	878	1223	1770	2720	268.61	226.39	126.4				287	765	0	
Mean	28	39	57	88	8.66	7.30	4.1				9.3	25	0	
RH = Relative Humidity														
ETp = Potential Evapotranspiration (Modified Penman Method)														

1.10 Climatic data for July 2019

DRAINAGE AND RECLAMATION INSTITUTE OF PAKISTAN (DRIP) CAMPUS, TANDO JAM														
METEOROLOGICAL DATA														
July, 2019														
Date	Average Daily Temp Co		RH %		Pan Evap. 24 hrs (mm)	ETP Daily (mm)	Wind Velocity Average Knot/hr	Wind Direction			Sunshine Hours		Rain Fall (mm)	Remarks
	Min.	Max.	Min.	Max.				9 A.M	12 noon	5 P.M	Hr.	Mint		
1	30	37	64	93	12.44	6.338	6.9	SSW	SSW	SSW	5	0		Could day day
2	30	37	64	93	7.36	7.359	4	SSW	SSW	SSW	10	35		
3	29	38	50	93	8.89	7.15	4	SSW	SSW	SSW	8	50		Could day day
4	30	37	59	86	9.14	7.339	5	SSW	SSW	SSW	8	30		Could day day
5	29	37	59	93	8.89	6.898	6.7	SSW	SSW	SSW	6	40		Could day day
6	30	37	74	93	7.87	5.601	6.5	SSW	SSW	SSW	4	50		Could day day
7	31	38	68	93	7.36	6.659	5.4	SSW	SSW	SSW	8	45		Could day day
8	31	38	59	93	8.38	7.681	6.6	SSW	SSW	SSW	8	40		Could day day
9	30	38	54	93	8.89	8.046	7.3	SSW	SSW	SSW	8	40		Could day day
10	30	38	54	86	9.65	8.194	7.8	SSW	SSW	SSW	8	30		Could day day
11	31	38	50	86	9.9	8.934	7.4	SSW	SSW	SSW	9	35		
12	31	36	58	86	11.43	8.701	7.4	SSW	SSW	SSW	10	0		
13	31	36	68	86	9.65	8.02	7.4	SSW	SSW	SSW	9	30		
14	31	38	63	86	11.43	6.664	7.6	SSW	SSW	SSW	4	0		Could day day
15	31	36	58	86	10.41	7.949	9.5	SSW	SSW	SSW	5	35		Could day day
16	30	36	58	93	10.16	7.318	8.6	SSW	SSW	SSW	6	15		Could day day
17	31	37	54	86	7.87	8.072	6.7	SSW	SSW	SSW	8	15		Could day day
18	29	37	59	93	8.63	7.23	5.8	SSW	SSW	SSW	8	30		Could day day
19	28	37	54	92	7.87	7.004	4.9	SSW	SSW	SSW	8	0		Could day day
20	28	38	63	93	6.6	7.177	2.7	SSW	SSW	SSW	11	0		
21	28	40	59	93	8.63	6.693	2	SSW	SSW	SSW	9	50		
22	31	40	47	86	7.36	6.143	1.9	SSW	SSW	SSW	6	30	18.3	Could day day
23	27	38	59	92	NIL	6.967	1.9	SSW	SSW	SSW	11	10		
24	30	38	54	86	11.17	7.205	3.1	SSW	SSW	SSW	9	30		
25	30	36	58	86	9.14	6.505	7.2	SSW	SSW	SSW	3	50		Could day day
26	30	37	54	86	10.92	8.674	8.3	SSW	SSW	SSW	8	30		Could day day
27	30	37	63	86	8.89	8.381	7.1	SSW	SSW	SSW	10	10		
28	30	38	58	86	9.9	6.047	6.7	SSW	SSW	SSW	2	25		Could day day
29	25	29	100	100	NIL	2.264	3.5	SSW	SSW	SSW	0	0	106.4	Could day day
30	27	34	93	100	NIL	4.231	1.8	SSW	SSW	SSW	5	30	2.5	Could day day
31	27	35	68	100	4.31	5.146	1.5	SSW	SSW	SSW	7	0		Could day day
Total	916	1146	1903	2804	253.14	216.59	173.2				221	785	127.2	
Mean	30	37	61	90	8.17	6.99	5.6				7.1	25	4.1	
RH = Relative Humidity														
ETp = Potential Evapotranspiration (Modified Penman Method)														

1.11 Climatic data for August 2019

DRAINAGE AND RECLAMATION INSTITUTE OF PAKISTAN (DRIP) CAMPUS, TANDO JAM														
METEOROLOGICAL DATA														
August, 2019														
Date	Average Daily Temp Co		RH %		Pan Evap. 24 hrs (mm)	ETP Daily (mm)	Wind Velocity Average Knot/hr	Wind Direction			Sunshine Hours		Rain Fall (mm)	Remarks
	Min.	Max.	Min.	Max.				9 A.M	12 noon	5 P.M	Hr.	Mint		
1	29	34	74	84	7.36	5.437	4.7	SSW	SSW	SSW	5	30		Could day day
2	27	34	74	92	6.09	6.185	5.1	SSW	SSW	SSW	8	10		Could day day
3	29	36	74	93	7.11	6.499	4.5	SSW	SSW	SSW	9	40		
4	29	37	68	93	8.38	5.699	4.5	SSW	SSW	SSW	6	5		Could day day
5	28	35	63	92	6.85	6.737	3.9	SSW	SSW	SSW	10	0		
6	28	35	68	92	8.12	6.965	5.3	SSW	SSW	SSW	10	20		
7	28	34	74	92	7.87	5.213	5	SSW	SSW	SSW	5	45		Could day day
8	28	36	63	92	6.09	5.847	3.7	SSW	SSW	SSW	7	0		Could day day
9	28	37	69	92	0.254	3.558	1.7	SSW	SSW	SSW	1	35	6.2	Could day day
10	28	34	79	100	Nil	3.877	1.3	SSW	SSW	SSW	4	0	43.2	Could day day
11	27	34	100	100	Nil	2.749	2.6	NNE	NNE	NNE	1	55	5	Could day day
12	25	34	86	100	Nil	4.784	3.3	SSE	SSE	SSE	7	40		Could day day
13	27	33	86	100	4.57	5.275	1.5	SSW	SSW	SSW	9	35		
14	27	34	89	92	3.81	4.812	2.3	SSW	SSW	SSW	7	0		Could day day
15	27	35	73	92	7.11	3.769	2.1	SSW	SSW	SSW	2	35		Could day day
16	27	33	73	92	5.58	4.237	3.9	SSW	SSW	SSW	3	0		Could day day
17	28	34	68	92	5.84	5.165	5	SSW	SSW	SSW	4	55		Could day day
18	27	34	79	92	4.82	6.283	4.2	SSW	SSW	SSW	10	30		
19	28	34	74	92	6.6	6.646	3.8	SSW	SSW	SSW	11	10		
20	27	34	74	92	6.6	6.603	3.6	SSW	SSW	SSW	11	30		
21	27	35	63	92	7.36	6.782	4	SSW	SSW	SSW	10	50		
22	27	35	63	92	7.11	7.384	5.5	SSW	SSW	SSW	11	15		
23	27	34	68	92	8.12	6.862	4.3	SSW	SSW	SSW	11	20		
24	28	35	73	92	8.12	7.035	5	SSW	SSW	SSW	11	20		
25	28	35	73	92	7.87	6.892	4.3	SSW	SSW	SSW	11	20		
26	27	37	59	92	8.12	7.138	3.5	SSW	SSW	SSW	11	15		
27	28	39	54	85	6.35	7.172	3.5	SSW	SSSW	SSW	9	50		
28	27	36	69	85	6.35	5.498	1.4	SSE	SSE	SSE	8	0	15.8	Could day day
29	27	29	92	100	Nil	2.701	1.5	SSW	NNE	NNE	1	40	12.4	Could day day
30	27	34	74	100	Nil	5.735	1.4	SSW	SSE	SSE	10	0		
31	28	35	80	100	4.31	5.533	0.7	SSW	SSW	SSW	9	0	3.3	
Total	853	1075	2276	2888	166.764	175.07	107.1				232	705	85.9	
Mean	28	35	73	93	5.38	5.65	3.5				7.5	23	2.8	
RH = Relative Humidity														
ETp = Potential Evapotranspiration (Modified Penman Method)														

1.12 Climatic data for September 2019

DRAINAGE AND RECLAMATION INSTITUTE OF PAKISTAN (DRIP) CAMPUS, TANDO JAM														
METEOROLOGICAL DATA														
September, 2019														
Date	Average Daily Temp Co		RH %		Pan Evap. 24 hrs (mm)	ETP Daily (mm)	Wind Velocity Average Knot/hr	Wind Direction			Sunshine Hours		Rain Fall (mm)	Remarks
	Min.	Max.	Min.	Max.				9 A.M	12 noon	5 P.M	Hr.	Mint		
1	27	36	74	92	5.08	4.677	1.4	SSW	SSW	SSW	7	0		Coulday Day
2	28	35	74	100	4.82	3.487	1	SSW	SSW	SSW	3	40		Coulday Day
3	28	35	68	92	5.08	5.578	1	SSW	SSW	SSW	10	30		
4	28	35	68	92	5.84	5.592	1.2	SSW	SSW	SSW	10	10		
5	28	37	64	85	6.85	5.42	2.1	SSW	SSW	SSW	8	20		Coulday Day
6	30	38	64	93	6.6	5.673	1.5	SSW	SSW	SSW	8	50		Coulday Day
7	30	37	68	86	8.63	5.499	1.5	SSE	SSE	SSE	8	35		Coulday Day
8	28	36	74	93	7.87	5.637	1.5	SSE	SSE	SSE	10	5		
9	29	37	68	86	7.87	5.802	0.8	SSE	SSE	SSE	10	30		
10	29	37	68	93	7.62	5.348	1.5	SSW	SSW	SSW	8	35		Coulday Day
11	28	37	64	92	5.84	6.269	3.1	SSW	SSW	SSW	10	10		
12	28	36	63	85	6.85	6.193	3.3	SSW	SSW	SSW	9	30		
13	28	36	68	92	7.36	5.895	4.7	SSW	SSW	SSW	8	10		Coulday Day
14	27	37	68	92	6.35	6.034	4.1	SSW	SSW	SSW	9	0		
15	27	38	63	85	7.87	6.74	4.3	SSW	SSW	SSW	10	0		
16	27	36	63	85	5.84	5.959	3.6	SSW	SSW	SSW	8	30		Coulday Day
17	27	35	68	85	6.85	6.421	4.2	SSW	SSW	SSW	10	30		
18	27	36	58	92	7.11	6.349	3.2	SSW	SSW	SSW	10	45		
19	26	39	55	92	4.06	6.096	1.7	SSW	SSW	SSW	10	35		
20	24	38	59	92	4.82	5.479	0.7	SEE	SEE	SEE	10	15		
21	27	38	59	92	8.89	5.634	0.4	SSW	SSW	SSW	10	15		
22	27	38	59	92	7.14	5.377	0.6	SSW	SSW	SSW	9	0		
23	27	38	59	92	5.08	5.634	0.4	SSW	SSW	SSW	10	15		
24	28	38	54	85	4.82	5.59	0.8	SSW	SSW	SSW	9	5		
25	27	37	59	92	5.08	5.298	0.6	SSW	SSW	SSW	9	0		
26	27	37	63	92	4.82	5.232	1.1	SSW	SSW	SSW	8	40	3	Coulday Day
27	27	36	63	92	4.57	5.659	1	SSW	SSW	SSW	10	45		
28	26	36	68	92	5.08	5.31	1	SSW	SSW	SSW	9	55		
29	27	36	68	92	5.08	4.522	0.7	SSW	SSW	SSW	7	50		Coulday Day
30	25	33	80	92	5.58	5.206	1.4	SSW	SSW	SSW	10	30		
Total	822	1098	1951	2717	185.35	167.61	54.4				267	715	3	
Mean	27	35	63	88	5.98	5.41	1.8				8.6	24	0.1	
RH = Relative Humidity														
ETp = Potential Evapotranspiration (Modified Penman Method)														

About the Authors



Dr. Altaf Ali Siyal is working as Professor and Head, Department of Integrated Water Resources Management (IWRM) in U.S.-Pakistan Center for Advanced Studies in Water (USPCAS-W) at Mehran University of Engineering & Technology (MUET), Jamshoro, Pakistan. Prior to this, he has worked as Incharge Dean, Faculty of Agricultural Engineering, and the Chairman Land & Water Management Department, at Sindh Agriculture University (SAU) Tandojam, Pakistan. In 2011, he got Endeavour Research Fellowship from the Australian Government for Postdoctoral Research on 'Soil, Water and Crop Environment' at CSIRO-ATSIP, Australia. During 2007-8, Dr. Siyal was awarded Fulbright Scholar Award for Post-Doctoral Research on 'Subsurface Irrigation Simulations' at University of California and the USDA-ARS Salinity Laboratory in Riverside, USA. He obtained Ph.D. in 2001 from the Cranfield University, UK on 'Maximizing salt leaching efficiency of aggregated clay saline soils' under Quaid-e-Azam Merit Scholarship sponsored by Ministry of Education, Government of Pakistan. He earned his Master's degree in Irrigation & Drainage in 1998 and Bachelor's degree in Agricultural Engineering in 1990 from the SAU Tandojam. Dr. Siyal received training on 'GIS and Remote Sensing Applications for the Water Sector' from UNESCO-IHE, Delft, Netherlands under the Netherlands Fellowship Program (NFP), and in Monitoring & Management of Natural Resources from the University of Maryland, USA, and SUPARCO, Pakistan. He has published more than 50 research articles, on soil, water, and irrigation related issues, in national and international journals. His field of interest is Water Resources Engineering & Management, Irrigation and Drainage, Soil Salinity and Land Reclamation, and GIS & Remote Sensing Applications in the management of water and other natural resources.





Dr. Chávez is an Associate Professor in the Civil and Environmental Engineering Department, and an Irrigation Specialist with Extension at Colorado State University. He has teaching, research, and extension responsibilities. His expertise is in irrigation water management, crop/vegetation water consumptive use (evapotranspiration, ET) determination and modeling, use of remote sensing for mapping ET, irrigation scheduling, irrigation systems design, irrigation systems efficiency, drainage and wetlands engineering, and precision irrigation. He teaches courses in Irrigation Systems Design, Irrigation Water Management, and Drainage and Wetlands Engineering subjects.



Main thrust of Applied Research component of the Water Center is to stimulate an environment that promotes multi-disciplinary research within the broader context of water-development nexus to support evidence-based policy making in the water sector. This is pursued using the framework provided by the six targets of the Sustainable Development Goal on Water i.e., SDG-6.

Contact:

U.S.-Pakistan Centers for Advanced Studies in Water
Mehran University of Engineering and Technology, Jamshoro-76062, Sindh - Pakistan

 92 22 210 9145  water.muett.edu.pk  /USPCASW  /USPCASW